

T-1997

SORPTION OF H₂S ON SPENT SHALE
IN PACKED BEDS

by
Enayatollah Pedram

ProQuest Number: 10782147

All rights reserved

INFORMATION TO ALL USERS

The quality of this reproduction is dependent upon the quality of the copy submitted.

In the unlikely event that the author did not send a complete manuscript and there are missing pages, these will be noted. Also, if material had to be removed, a note will indicate the deletion.



ProQuest 10782147

Published by ProQuest LLC (2018). Copyright of the Dissertation is held by the Author.

All rights reserved.

This work is protected against unauthorized copying under Title 17, United States Code
Microform Edition © ProQuest LLC.

ProQuest LLC.
789 East Eisenhower Parkway
P.O. Box 1346
Ann Arbor, MI 48106 – 1346

A Thesis submitted to the Faculty and the Board of Trustees of the Colorado School of Mines in partial fulfillment of the requirements for the degree of Master of Science, Chemical and Petroleum Refining.

Signed: E. Pedram
E. Pedram

Golden, Colorado

Date: Nov. 30, 1977

Approved: A.L. Hires
A.L. Hires
Thesis Advisor

Philip F. Dickson
Philip F. Dickson
Head of Chemical and
Petroleum Refining
Department

Golden, Colorado

Date: Dec. 1, 1977

ABSTRACT

ARTHUR LAKES LIBRARY
COLORADO SCHOOL of MINES
GOLDEN, COLORADO 80401

This study includes the adsorption of H_2S on oil shale that had been retorted for two hours at various temperatures ranging from 300 to 1000°C. An experimental flow adsorption apparatus was designed and constructed, and breakthrough curves were obtained at 10, 25, and 60°C. Gas concentrations of 1000, 2000, 3000, 5000, 7000, and 10,000 ppm H_2S in dry nitrogen were used. Equilibrium isotherms were calculated from the adsorption data and were modeled by the Langmuir, Freundlich, and Dubinin-Polanyi equations. Experimental breakthrough curves were compared with a theoretical model of the flow system and diffusion coefficients were estimated at 10, 25, and 60°C for the concentrations 1000, 5000, and 10,000 ppm H_2S in nitrogen.

TABLE OF CONTENTS

	<u>Page</u>
Abstract -----	iii
List of Figures -----	vi
List of Tables -----	ix
Introduction -----	1
Theory -----	4
Equilibrium Considerations -----	4
Mass Transfer Mechanisms -----	11
Retorting Experiment -----	16
Apparatus -----	16
Procedure -----	16
Adsorption Study -----	19
Apparatus -----	19
Procedure -----	24
Results and Discussion -----	26
Adsorption -----	26
Diffusion Coefficients -----	69
Energy of Activation -----	78
Heat of Adsorption -----	81
Conclusion -----	82
Nomenclature -----	85
Bibliography -----	88
Appendix I. Sample Calculation - BET Surface Area -----	90
II. Details of the Computer Program for Langmuir Type of Isotherms -----	92
III. Details of the Computer Program for Freundlich Type of Isotherms -----	94

Table of Contents continued

	<u>Page</u>
Appendix IV. Details of the Computer Program for Dubinin-Polanyi Type of Isotherms -----	96
V. Sample Calculation - Dubinin- Polanyi Equation -----	98
VI. Sample Calculation - Uptake of H ₂ S on Spent Shale -----	100
VII. Parameters Used in Calculations -----	101
VIII. Values of Q ₁ C ₀ for Theoretical Breakthrough Curve (output of program) ----	102
IX. Experimental Breakthrough, Curve Data -----	111

LIST OF FIGURES

	<u>Page</u>
Figure 1. The Piping Schematic of Retorting Apparatus--	18
2. The Flowmeter Calibration-Scale Reading vs. Flow Rate of Tube No. 2 -----	20
3. The Flowmeter Calibration-Scale Reading vs. Flow Rate for Tube No. 1 -----	21
4. The Piping Schematic of Adsorption Apparatus -----	23
5. The BET Surface Area of the Spent Shale Retorted for Two Hours at Different Temperatures Ranging from 350 to 950°C-----	29
6. Adsorption at 7°C of H ₂ S on Spent Shale at 7°C for Shale Retorted at Temperatures Ranging from 350 to 950°C -----	32
7. Comparison of Experimental Breakthrough Curve for Concentrations of 1000, 2000, 3000, 5000, and 10,000 PPM H ₂ S in Nitrogen at 10°C-	34
8. Comparison of Experimental Breakthrough Curves for Concentrations of 1000, 2000, 3000, 5000, 7000, 10,000 PPM H ₂ S in Nitrogen at 25°C -----	35
9. Comparison of Experimental Breakthrough Curves for Concentrations of 1000, 2000, 3000, 5000, 7000, and 10,000 PPM H ₂ S in Nitrogen at 60°C -----	36
10. Comparison of Breakthrough Curves for the Concentration 10,000 PPM H ₂ S in Nitrogen at 10°C, 25°C, and 60°C-----	38

List of Figures continued

	<u>Page</u>
Figure 11. Comparison of Breakthrough Curves for the Concentration 7000 PPM H ₂ S in Nitrogen at 10°C, 25°C, and 60°C -----	39
12. Comparison of Breakthrough Curves for the Concentration 5000 PPM H ₂ S in Nitrogen at 10°C, 25°C, and 60°C -----	40
13. Comparison of Breakthrough Curves for the Concentration 3000 PPM H ₂ S in Nitrogen at 10°C, 25°C, and 60°C -----	41
14. Comparison of Breakthrough Curves for the Concentration 2000 PPM H ₂ S in Nitrogen at 10°C, 25°C, and 60°C -----	42
15. Comparison of Breakthrough Curves for the Concentration 1000 PPM H ₂ S in Nitrogen at 10°C, 25°C, and 60°C -----	43
16. Equilibrium Isotherms for Adsorption of H ₂ S on Spent Shale at 10°C, 25°C, and 60°C Fit to the Langmuir Equation -----	46
17. Adsorption Isotherms of H ₂ S on Spent Shale at 10°C Plotted According to the Langmuir Equation (Testing of the Langmuir Equation)-----	51
18. Adsorption Isotherms of H ₂ S on Spent Shale at 25°C Plotted According to the Langmuir Equation (Testing of the Langmuir Equation)-----	52
19. Adsorption Isotherms of H ₂ S on Spent Shale at 60°C Plotted According to the Langmuir Equation (Testing of the Langmuir Equation)-----	53
20. Equilibrium Isotherms for Adsorption of H ₂ S on Spent Shale at 10°C, 25°C, and 60°C Fit to the Freundlich Equation -----	56
21. Adsorption Isotherms of H ₂ S on Spent Shale at 10°C Plotted According to the Freundlich Equation (Testing of the Freundlich Equation) -----	57

Table of Figures continued

	<u>Page</u>
Figure 22. Adsorption Isotherms of H ₂ S on Spent Shale at 25°C Plotted According to the Freundlich Equation (Testing of the Freundlich Equation) -----	58
23. Adsorption Isotherms of H ₂ S on Spent Shale at 60°C Plotted According to the Freundlich Equation (Testing of the Freundlich Equation)-----	59
24. Characteristic Curve for the Adsorption of H ₂ S on the Spent Shale -----	61
25. Plot of Log x vs. [Log ₁₀ (P ₀ /P)] ² for the Adsorption of H ₂ S at 10°C on Spent Shale Plotted According to the Dubinin Equation (Potential Theory)-----	66
26. Plot of Log x vs. [Log ₁₀ (P ₀ /P)] ² for the Adsorption of H ₂ S at 25°C on Spent Shale Plotted According to the Dubinin Equation (Potential Theory)-----	67
27. Plot of Log x vs. [Log ₁₀ (P ₀ /P)] ² for the Adsorption of H ₂ S at 60°C on Spent Shale Plotted According to the Dubinin Equation (Potential Theory) -----	68
28. The Theoretical Breakthrough Curve for Q ₁ C ₀ = 4.03 -----	70
29. The Theoretical Breakthrough Curve for Q ₁ C ₀ = 6.12 -----	71
30. The Theoretical Breakthrough Curve for Q ₁ C ₀ = 8.64 -----	72
31. Comparison of Diffusion Coefficients at 10°C, 25°C, and 60°C -----	77
32. Effective Diffusivity vs. (1/T)x10 ³ -----	80
33. Equilibrium Isosteres for Calculation Heat of Adsorption -----	82

LIST OF TABLES

	<u>Page</u>
Table 1. X-ray Diffraction Analysis of Shale Samples Retorted for Two Hours -----	27
2. The BET Surface Area of Oil Shale Retorted for Two Hours -----	28
3. Chemical Analysis of Oil Shale Retorted for Two Hours -----	30
4. Adsorption of H ₂ S on Spent Shale at 7°C Using a Concentration of 10,000 PPM H ₂ S in Nitrogen Gas -----	31
5. Equilibrium Isotherm Data and Langmuir Constants for H ₂ S on Spent Shale -----	45
6. Equilibrium Adsorption Quantities of H ₂ S at 10°C on Spent Shale Retorted at 750°C-----	47
7. Equilibrium Adsorption Quantities of H ₂ S at 25°C on Spent Shale Retorted at 750°C-----	48
8. Equilibrium Adsorption Quantities of H ₂ S at 60°C on Spent Shale Retorted at 750°C-----	49
9. Equilibrium Isotherm Data and Freundlich Constants -----	55
10. Data for Calculation of Polanyi-Dubinin Theory at Temperature of 10°C-----	62
11. Data for Calculation of Polanyi-Dubinin Theory at Temperature of 25°C -----	63
12. Data for Calculation of Polanyi-Dubinin Theory at Temperature of 60°C -----	64
13. Diffusion Coefficients at 10°C of H ₂ S Through Spent Shale for Concentrations of 1000, 5000, and 10,000 PPM of H ₂ S in Dry Nitrogen -----	74

List of Tables continued

	<u>Page</u>
Table 14. Diffusion Coefficients at 25°C of H ₂ S Through Spent Shale for Concentrations of 1000, 5000, and 10,000 PPM of H ₂ S in Dry Nitrogen -----	75
15. Diffusion Coefficients at 60°C of H ₂ S Through Spent Shale for Concentrations of 1000, 2000, 5000, and 10,000 PPM of H ₂ S in Dry Nitrogen -----	76
16. Experimental Parameters of Eq. 44 -----	79
17. Heat of Adsorption at Different Loading Points -----	81
18. Desorption by Pure Nitrogen of H ₂ S from Spent Shale Particles at 10°C 25°C, and 60°C -----	84

ACKNOWLEDGEMENTS

I am indebted to Dr. Anthony L. Hines, my thesis advisor, for giving me the opportunity to work on this project and for his many useful suggestions during the preparation of this thesis.

I am also grateful to Dr. William D. Copeland, Dean of the Graduate School, and Dr. Philip F. Dickson, Professor and Head of the Department of Chemical and Petroleum Refining for their guidance while at the Colorado School of Mines.

Also the support of the United States Energy Research and Development Administration under contract number E(29-2)-3780 is gratefully acknowledged.

Last, but certainly not least, I express my gratitude to my wife, Vida, for her moral support at a time when it was most needed.

INTRODUCTION

Oil shale is the term applied to fine-grained sedimentary rocks which contain appreciable quantities of an organic material called Kerogen. The solid waste material remaining after retorting is called spent shale.

The present study indicates that oil shale is a highly consolidated organic-inorganic system with no significant micropore structure, pore volume, or internal surface. The mineral constituents have an appreciable surface area of about 3 to 5 square meters per gram (1), which appears to be limited mainly to external surface.

In-situ retorting of oil shale involves the in-place heating and retorting of an underground shale formation under conditions wherein the flows of heat, vapors, and liquids remain under control, resulting in the recovery of acceptable quantities of gaseous and liquid products from the shale. The in-situ method eliminates mining the shale and the pollution problems that accompany the disposal of the spent shale.

One design of a 50,000 barrel per day in-situ process indicates an air requirement in excess of 4 million scfm.

Consequently, the raw untreated exhaust gas flow for steady shale operation is predicted to be about 4.5 million scfm and will contain low concentrations of hydrogen sulfide gas, 1000 parts per million H₂S by volume (2).

Also a gas analysis of the controlled state retort at the Laramie Energy Research Center indicates that a 50,000 barrel per day process would yield about 64,000 tons per year of H₂S (2). This value is considerably larger than should be expected from a normal in-situ process because the controlled state retort is heated electrically instead of by combustion. The combustion process will convert a large portion of the H₂S to SO₂. A number of commercially available H₂S removal systems are presently used in the natural gas industry. Although the USBM has been successful in removing low concentrations of H₂S, the dilute H₂S composition, in conjunction with large volumes of low pressure exhaust gas poses a number of technical problems.

At the retorting temperatures in the presence of water, the carbon that remains in the shale should be activated to some extent and should provide an effective adsorbent for hydrocarbon and combustion gases. In this work, the adsorption of H₂S was investigated under steady flow conditions by using spent shale as an adsorbent in a packed bed. Packed bed studies were made to determine breakthrough

curves and to obtain an estimate of equilibrium isotherms at atmospheric pressure. The parameter variations included adsorbate concentration, temperature, and bed height. Flow-rate was maintained constant throughout the runs. Diffusion coefficient were calculated from the breakthrough curves by considering models of the packed bed and the equilibrium data.

The raw shale samples used in the retort were obtained from Laramie, Wyoming, and were to be processed in their 150 ton retort. The particular material used contained 35 gallons of oil per ton of shale as found by modified Fischer assay at the Laramie facility. In order to study the effects of retorting temperature on the properties of the spent shale, samples of raw shale were prepared so that the effects of retorting temperatures would not be masked by variations in properties of the shale. This was done by grinding a large quantity of raw shale and collecting samples that passed a one-fourth inch screen and was collected on a one-eighth inch screen; the collected shale was mixed several times to provide a homogeneous sample.

THEORY

The main subject of this study is the adsorption of H_2S on retorted oil shale in a steady flow system with the goal of determining adsorption isotherms, the rate of adsorption, and the diffusion coefficients of H_2S through spent shale.

In general the types of isotherms and a mathematical model for evaluating the diffusion coefficients will be discussed in this section.

Equilibrium Considerations

When the pressure or concentration of the gas is varied and temperature is kept constant, the amount of adsorbed gas plotted against the pressure or concentration of the gas is called the adsorption isotherm (see Figure 16). An isotherm may have one of five general forms: type one is associated with simple formation of a monolayer of molecules adsorbed, types two and three are associated with the formation of multilayers, and types four and five are characteristics of multilayer adsorption on highly porous adsorbents. Since a highly porous adsorbent was not used, discussion will be limited only to types one and two.

The Freundlich Theory

The first theory, often referred to as classical theory, for the type one isotherm was proposed by Freundlich. Although it is the oldest theory, it is still widely used in industrial practice. In addition to unimolecular adsorption, other assumptions involved with this theory are:

- a) The heat of adsorption is not the same on the surface of adsorbent--it decreases due to the heterogeneity.
- b) The heat of adsorption is small at low surface coverage because in dilute layers the adsorbed molecules tend to be too far apart for repulsions to be appreciable.
- c) The adsorption varies with a power of the pressure that is smaller than one but greater than zero.

The Freundlich isotherm equation is:

$$q^* = m(C^*)^{1/n}, \quad n > 1 \quad \text{Eq. (1)}$$

where q^* is the amount adsorbed and m and n are quantities dependent on temperature and C^* is the gas concentration.

To test whether a set of experimental data obeys the Freundlich isotherm model, Eq. (1) can be written in linear form as

$$\log q^* = \log m + \frac{1}{n} \log C^* \quad \text{Eq. (2)}$$

If the graph of $\log q^*$ versus $\log C^*$ gives a straight line, the adsorption data obeys the Freundlich equation with the slope equal to $1/n$ and with the intercept equal to $\log m$.

The Langmuir Theory

The second theory for a type one isotherm was proposed by Langmuir (4) in 1915 and is perhaps the most important single theory in the field of adsorption. This theory includes the following assumptions:

- a) The formation of a monolayer.
- b) Adsorption is localized and takes place only through collisions of gas molecules with vacant sites.
- c) Each site can accommodate one and only one molecule.
- d) The energy of an adsorbed molecule is the same anywhere on the surface and is independent of the presence or absence of nearby adsorbed molecules.

The Langmuir Isotherm equation is:

$$q^* = \frac{Q_0 C^*}{1 + Q_1 C^*} \quad \text{Eq. (4)}$$

where: Q_0 is first Langmuir Constant, dimensionless, Q_1 is second Langmuir Constant, cm^3/gm ., C^* is the gas concentration, gm/cm^3 and q^* is equilibrium

adsorbate concentration gm/cm³.

The test of whether a set of experimental data obeys the Langmuir isotherm equation is done by arranging Eq. (4) in linear form as

$$\left(\frac{1}{q^*}\right) = \left(\frac{1}{Q_0}\right) \left(\frac{1}{C^*}\right) + \left(\frac{Q_1}{Q_0}\right) \quad \text{Eq. (5)}$$

A plot of $\frac{1}{q^*}$ against $\left(\frac{1}{C^*}\right)$ gives a straight line with a slope $\left(\frac{1}{Q_0}\right)$ and an intercept of $\left(\frac{Q_1}{Q_0}\right)$. It must be emphasized, however, that obtaining a satisfactory straight line is a necessary but not a sufficient condition for the applicability of Langmuir's theory to the data in question.

The Potential Theory (Type Two Isotherm)

These types of isotherms are characteristic of multi-layer adsorption on uniform surfaces. One of the theories that was proposed for this type of isotherm is the potential theory by Polanyi (5), (6).

The adsorbent exerts a strong attractive force upon the gas in its vicinity and this attraction gives rise to adsorption. The attraction forces reaching out from the surface are so great that many adsorbed layers can form on the surface. These layers are under compression, partly because of the attractive forces of the surface and partly because each layer is compressed by the other layers adsorbed

on top of it. The compression is the greatest on the first adsorbed layer, less on the second, and so on until the density decreases to that of the gas. The assumptions involved in the Polanyi theory are as follows.

- a) Adsorption is due to long range attractive forces extending out from the adsorbent surface.
- b) The gas obeys the same equation of state in the adsorbed phase as in the gas phase.
- c) The adsorption potential is similar to the gravitational potential.
- d) The curve $\epsilon = f(\theta)$ is the same for all temperatures. The curve is a distribution curve or characteristic curve, where θ is the adsorbed phase according to the potential theory and ϵ is the adsorption potential.

Polanyi made no attempt to derive an expression for the adsorption isotherm from the potential theory, but this has been done by Dubinin (7). The adsorption potential, resulting as it does from the dispersion and polar forces between the solid and the adsorbate molecules, is independent of temperature but varies according to the nature of the adsorbate as well as that of the solid.

Dubinin and his co-workers (7) (8) advanced arguments favoring the view that the volume of the adsorption space may be expressed as a Gaussian function of the corresponding

adsorption potential by the relation

$$W = W_0 e^{-k(\epsilon/\beta)^2} \quad \text{Eq. (6)}$$

where: β is a constant ratio termed by Dubinin as the affinity coefficient,
 W_0 is the total volume of all the micropores,
 W is volume of the gas adsorbed, and
 k is a constant characterizing the pore size distribution.

Both W and ϵ can, of course, be calculated from the experimental adsorption isotherm, so that both sides of the equation can be evaluated

$$W = f(\epsilon) \quad \text{Eq. (7)}$$

For an equilibrium pressure P , the adsorption potential at the surface (ϵ) is given by

$$\epsilon = R T \ln \frac{P_0}{P} \quad \text{Eq. (8)}$$

Where P_0 is the saturated vapor pressure of the adsorbate.

The volume W will be given by

$$W = \frac{x}{\rho} \quad \text{Eq. (9)}$$

where x is the adsorption in grams corresponding to the pressure P , and ρ is the density of the fluid.

Upon substitution for W and for ϵ in Eq. (6), this may be rewritten in the linear form

$$\log_{10} x = \log_{10} (W_0 \rho) - (2.303 \frac{k}{\beta^2} (RT)^2) (\log_{10} P_0/P)^2 \quad \text{Eq. (10)}$$

Thus a plot of $\log x$ versus $[\log_{10} (P_0/P)]^2$ should give a straight line with a slope of $[2.303 \frac{k}{\beta^2} (RT)^2]$ and with the intercept, $\log_{10} (W_0 \rho)$.

Dubinin's treatment has been modified by Kaganer (9) to yield a method for the calculation of specific surface from the isotherm. He confines attention to the monolayer region, and assumes that it is the distribution of adsorption potential over the sites on the surface which is Gaussian in type, and so can be represented in the linear form by the equation

$$\log_{10} x = \log (x_m) - [2.303 k_1 R^2 T^2] (\log_{10} \frac{P_0}{P})^2 \quad \text{Eq. (11)}$$

where: k_1 is a constant which characterizes the Gaussian distribution. Equation (11) is identical in form with Dubinin's Eq. (10), and a plot of $\log_{10} x$ versus $(\log_{10} \frac{P_0}{P})^2$ should again give a straight line; but the intercept on the ordinate axis (where $[\log_{10} (\frac{P_0}{P})]^2 = 0$, or $P=P_0$) is now equal to the logarithm of the monolayer capacity rather than to the logarithm of the pore volume. The method should, therefore, yield a value of the specific surface, and it is claimed that it can be applied in the low pressure region, below relative pressures of 10^{-4} .

Determination of Surface

The standard method for measuring the solid surface areas is based on the adsorption of a gas on the solid

surface. Usually the amount of nitrogen adsorbed at equilibrium at the normal boiling point (-195.8 C) is measured over a range of nitrogen pressures below 1 atm. Under these conditions several layers of molecules may be adsorbed on top of each other on the surface. The amount adsorbed when one molecular layer is attained must be identified in order to determine the area. To determine the absolute surface area by the Brunauer-Emmett-Teller method (10) it is necessary to select a value for the area covered by one adsorbed molecule. This is,

$$S_g = \left(\frac{V_m N_0}{V} \right) \cdot \alpha \quad \text{Eq. (12)}$$

where $\alpha = 1.09 \left[\frac{M}{N_0 \rho} \right]^{2/3}$, M is molecular weight and ρ is the density of the adsorbed molecules (11). V_m is Volume of one monomolecular layer of gas, N_0 is Avogadro's number, 6.02×10^{23} molecules mole, and V is the volume per mole of gas at conditions of V_m . Since V_m is recorded at standard temperature and pressure $V = 22,400$ (cm³/g mole). The term in brackets represents the number of molecules adsorbed. If V_m is based on a 1.0 gram sample; then S_g is the total surface per gram of solid adsorbent.

The other three types of isotherm will not be discussed here because the experimental equilibrium data are not of that shape.

Mass Transfer Mechanisms

An overall mass balance, an equilibrium relationship between the adsorbate concentration in the gas phase to

that in the adsorbent phase and the rate of adsorption are necessary to describe adsorption behavior. To model the system, a material balance is made over a differential element ΔZ in the fixed bed with the following assumptions:

Constant density, the fluid velocity is uniform over the bed cross section, and the particles and void spaces in the bed contain no adsorbate initially. If it is also assumed that axial diffusion is negligible, then the material balance becomes

$$\frac{\partial C}{\partial t} + v \frac{\partial C}{\partial Z} = - \frac{1}{m} \frac{\partial q}{\partial t} \quad \text{Eq. (13)}$$

ARTHUR LAKES LIBRARY
 COLORADO SCHOOL of MINES
 GOLDEN, COLORADO 80401

This equation may be simplified by a change of variables.

$$X = \frac{Z}{mv}, \quad \theta = t - \frac{Z}{v} \quad \text{Eq. (14)}$$

$$\frac{\partial C}{\partial t} = \frac{\partial C}{\partial X} \cdot \frac{\partial X}{\partial Z} \cdot \frac{\partial Z}{\partial t} = \frac{1}{mv} \left(\frac{\partial Z}{\partial t} \right) \cdot \left(\frac{\partial C}{\partial X} \right) \quad \text{Eq. (15)}$$

$$\frac{\partial C}{\partial Z} = \frac{\partial C}{\partial X} \cdot \frac{\partial X}{\partial Z} = \frac{1}{mv} \left(\frac{\partial C}{\partial X} \right) \quad \text{Eq. (16)}$$

$$\frac{\partial q}{\partial t} = \left(\frac{\partial q}{\partial \theta} \right) \cdot \left(\frac{\partial \theta}{\partial t} \right) = \left[1 + \frac{1}{v} \frac{\partial Z}{\partial t} \right] \cdot \frac{\partial q}{\partial \theta} \quad \text{Eq. (17)}$$

If we insert Equations (14), (15), (16), and (17) into Eq. (13), the result is

$$\frac{\partial C}{\partial X} = - \left(\frac{\partial q}{\partial \theta} \right) \quad \text{Eq. (18)}$$

The appropriate boundary and initial conditions are given in Eqs. (19) and (20).

$$C(0, \theta) = C_0 \quad \text{Eq. (19)}$$

$$q(X, 0) = 0 \quad \text{Eq. (20)}$$

The solid phase balance is the usual transient diffusion equation for a sphere. This may be expressed as:

$$\frac{\partial q_i}{\partial t} = D \nabla^2 q_i \quad \text{Eq. (21)}$$

This equation is usually used for diffusion in solids or stationary liquids ($v = 0$). Equation (21) can be written in spherical coordinates as follows

$$\frac{\partial q_i}{\partial t} = \frac{D}{r^2} \frac{\partial}{\partial r} \left(r^2 \frac{\partial q_i}{\partial r} \right) \quad \text{Eq. (22)}$$

The appropriate boundary and initial conditions are given below,

$$\text{I.C. \#1, } q_i(X, r, 0) = 0 \quad 0 \leq r < R_1, X \geq 0$$

$$\text{B.C. \#1, } \frac{\partial q_i(X, 0, \theta)}{\partial r} = 0, \theta = t = 0$$

$$\text{B.C. \#2, } X = 0, C = C_0 \text{ and } \theta = t = 0$$

The overall adsorbate accumulation of the particles averaged over the particle volume is represented by

$$q(X, \theta) = \frac{3}{R_1^3} \int_0^{R_1} q_i(X, r, \theta) r^2 dr \quad \text{Eq. (23)}$$

In a more recent study carried out by Antonson (12), the above equations were solved by assuming that the experimental isotherm data could be fit by the Langmuir model. If we insert the Langmuir isotherm equation into equation (23), then

$$q(x, \theta) = 3/R_1^3 \int_0^{R_1} \left[\frac{Q_0 C^*}{1+Q_1 C^*} \right] \cdot r^2 \cdot dr \quad \text{Eq. (24)}$$

This system of equations can be reduced to a single integro-differential equation by use of Duhamel's theorem and suitable manipulations of equations (13) to (23). The final result is

$$\frac{\partial \theta}{\partial X_{(2)}} = -2 \sum_{n=1}^{n=\infty} \int_0^{\theta_{(2)}} \frac{\partial f}{\partial \lambda} \exp \left[-\frac{1}{2} n^2 \cdot \pi^2 \cdot [\theta_{(2)} - \lambda] \right] d\lambda \quad \text{Eq. (25)}$$

$$\text{where } f(\theta) = \frac{\theta}{1+Q_1 \cdot C_0 \cdot \theta} \quad \text{Eq. (26)}$$

$$X_{(2)} = \frac{3D \cdot Q_0 \cdot X}{R_1^2} = \frac{3D \cdot Q_0 \cdot Z}{mv \cdot R_1^2} \quad \text{Eq. (27)}$$

$$\theta_{(2)} = \theta_{(1)} = \dots \quad \text{Eq. (28)}$$

where: $X_{(i)}$ is dimensionless column length variable

($i = 1, 2, 3,$)

$\theta_{(i)}$ is dimensionless time variable

$\theta = C/C_0$ dimensionless concentration

Finite difference techniques offer the best alternative for solution. It has been solved numerically by Antonson's (12) to yield a solution for $C(X, \theta)$ in terms of the following three dimensionless parameters.

$$\theta = t - \frac{Z}{v} \quad \text{Eq. (29)}$$

$$\frac{\theta T}{\eta} = (2 m v / 3 Q_0 Z) \theta \quad \text{Eq. (30)}$$

For each run, (C/C_0) should be plotted as a function of time on semilog tracing paper. Each resultant breakthrough curve will be superimposed on the theoretical curves and will be adjusted until the theoretical curve which most closely approximates it is found. The parameter η which corresponds to the best fit will be used to calculate the intraparticle diffusivity.

$$D = \left(\frac{mv R^2}{3Q Z} \right) \eta \quad \text{Eq. (31)}$$

Previous investigators (3) have found that the dependence of intraparticle diffusivity on temperature could be adequately expressed by an Arrhenius type of relation; that is

$$D = D_0 \exp(- Q/R T) \quad \text{Eq. (32)}$$

Hence by plotting $\ln(D)$ versus $(1/T)$ for runs at the same adsorbate concentration but different bath temperatures, D_0 and Q/R can be evaluated. The best line through the experimental data is obtained by the method of least squares. The slope of this line is $(- Q/R)$ while the intercept is $\ln(D_0)$.

RETORTING EXPERIMENT

Apparatus

The experimental equipment used in this study consisted of a two-foot long stainless steel retort vessel with an inside diameter of 2 inches. The retort was sealed with threaded caps that had been tapped at each end to allow for the removal of oil and combustion gases produced from the shale and to provide an inert atmosphere, while retorting by passing nitrogen through the system. The system is also equipped with: a safety relief valve, a check valve, a special electrical furnace with a digital temperature controller, an electrical resistor with its heating tape for keeping the tubes warm, a flowmeter, a vessel for collection of the oil product, a cooling bath for cooling the produced gas and oil, and the necessary piping and valves.

A drawing of the experimental apparatus is shown in Figure (1).

Procedure

The oil shale samples used in the retort were obtained from Laramie, Wyoming, and were prepared to provide a homogeneous sample. This was done by grinding a large quantity

of raw shale such that it passed a one-fourth inch screen and was collected on a one-eighth inch screen. The collected shale was then mixed several times to obtain a homogeneous sample. The retort vessel was filled with the crushed raw shale, the retort was placed in the electrical furnace, and the tubes were connected. During retorting, inert nitrogen gas was passed through the retort vessel at the rate of 100 cm³/min. to provide an inert atmosphere.

After constructing the system, the electrical power line was connected and temperature was set to the desired value. After the retort reached the desired temperature, retorting was done for two hours. The retort vessel and the sample was cooled to ambient temperature while continuing the nitrogen flow. The solid waste material remaining after retorting, spent shale, was crushed and sieved to the desired size, 16 to 40 U.S. mesh.

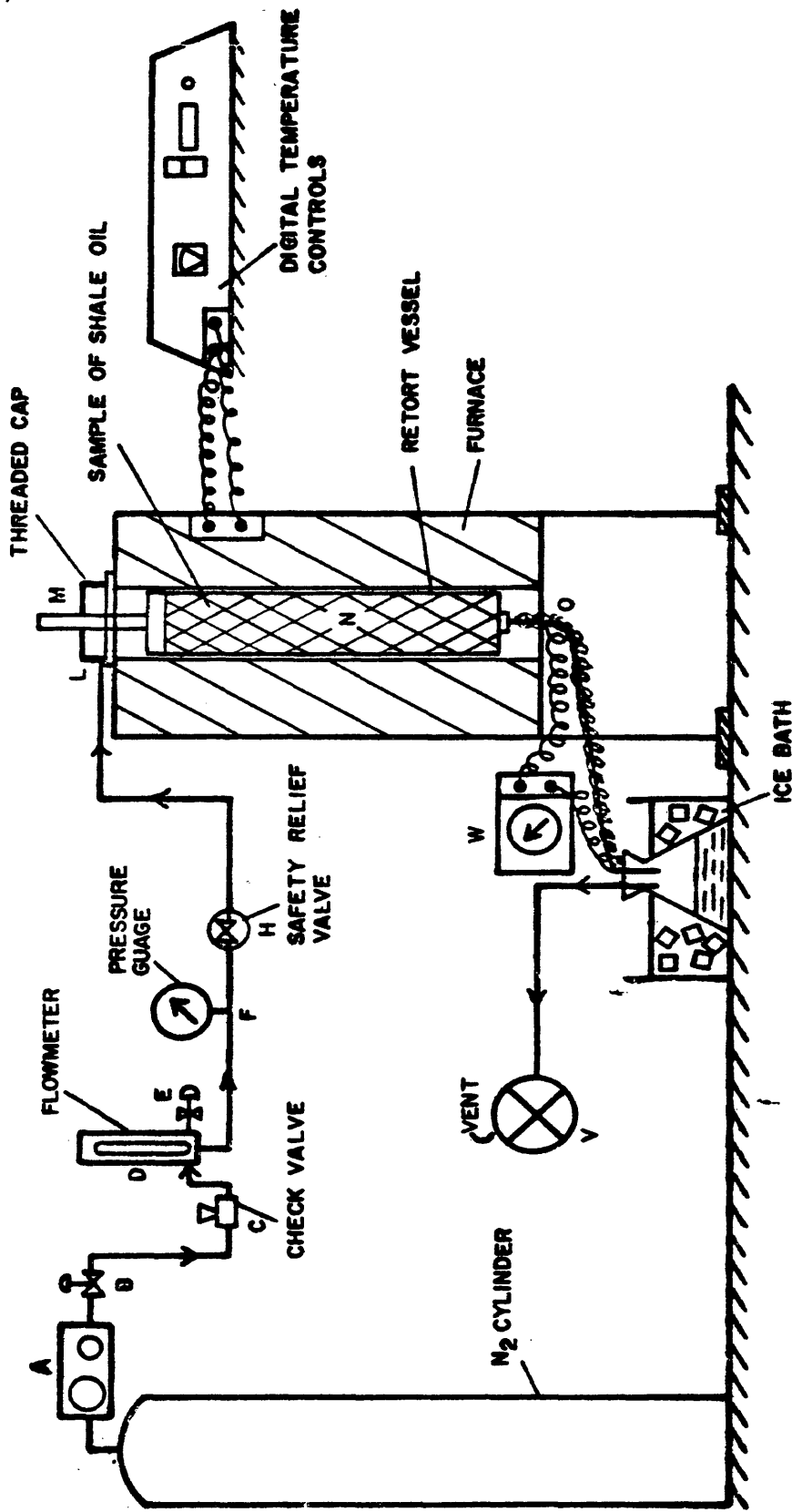


FIGURE 1. THE PIPING SCHEMATIC OF RETORTING APPARATUS.

ADSORPTION STUDY

Apparatus

The experimental apparatus used in this study consisted of the following equipment: cylinders containing prepared gas mixtures with concentrations of 1000, 2000, 3000, 5000, 7000, and 10,000 ppm H₂S in nitrogen, a nitrogen cylinder for desorption of adsorbent, a 6-inch long stainless steel column with an inside diameter of 1/2 in. containing the adsorbent, a safety relief valve, four check valves, a needle control valve, an injector valve, a constant-temperature bath with electronic relay, and a flowmeter. Also used in the system was a Beckman model 25 ultraviolet spectrophotometer detector, which is capable of measuring light at wave-lengths from 190 to 700 manometers, with its recorder and special UV silica cell which was installed at the exit of the flow line. The light intensity changed with any change in the gas concentration and the results were recorded as a function of time.

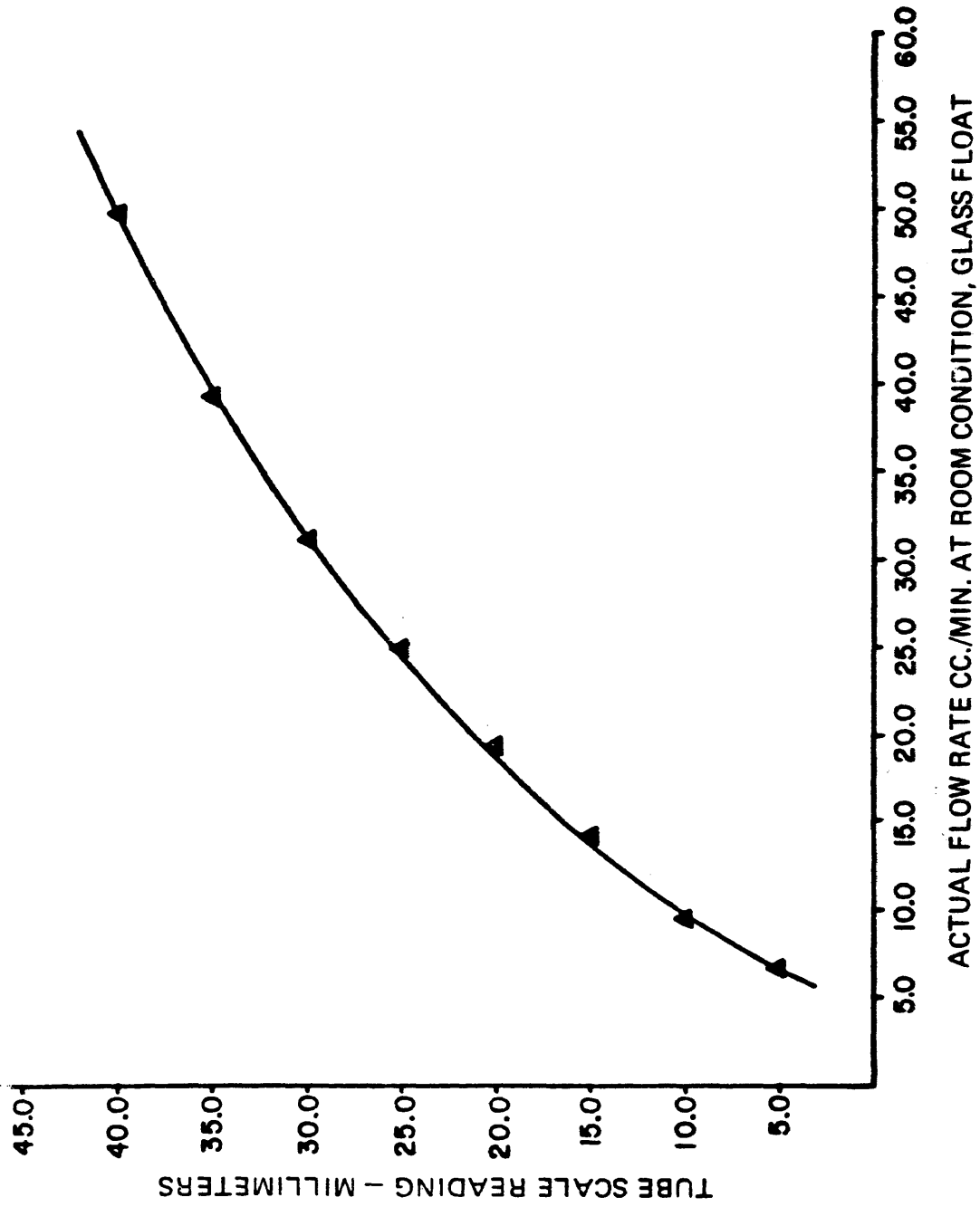


FIGURE 2. The Flowmeter Calibration-Scale Reading vs. Flow Rate of Tube No. 2.

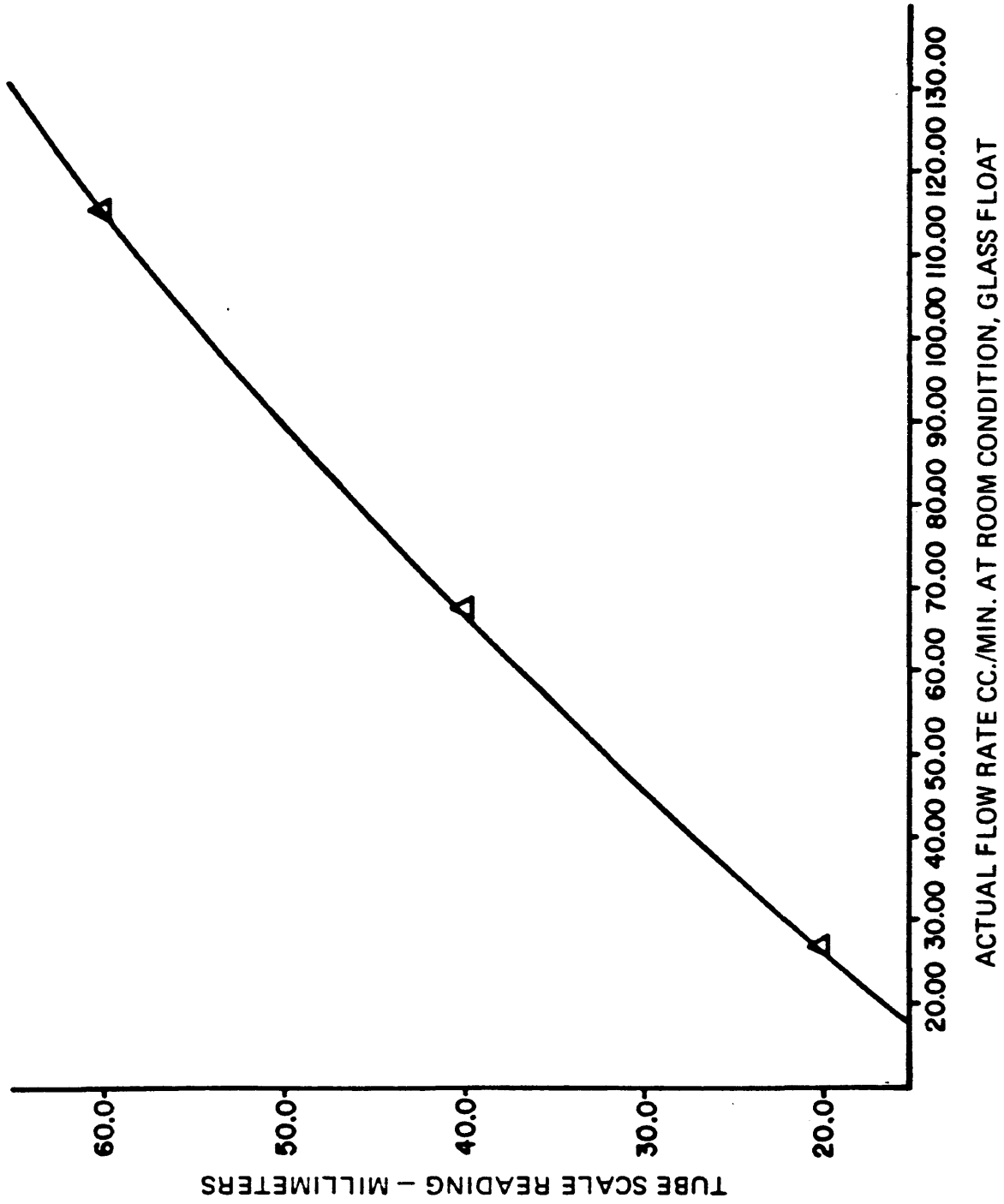


FIGURE 3. THE FLOWMETER CALIBRATION-SCALE READING VS. FLOW RATE FOR TUBE NO. 1.

A drawing of the experimental apparatus is shown in Fig. (4). The flowmeter was calibrated by a soap bubble flowmeter. The calibration curves for tube #1 and tube #2 of the flowmeter were obtained and are shown in Figure (2) and Figure (3).

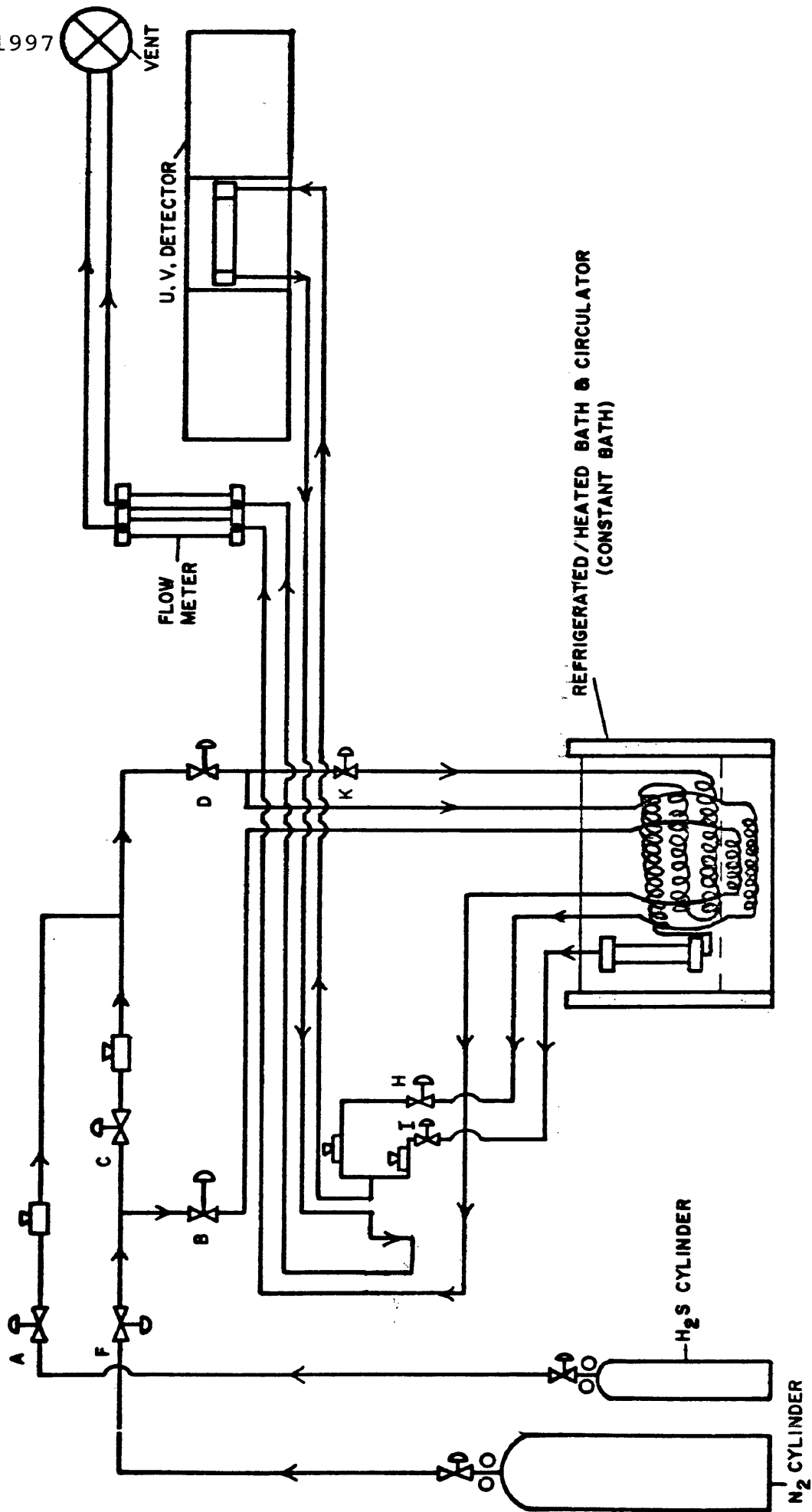


FIGURE 4. THE PIPING SCHEMATIC OF ADSORPTION APPARATUS.

Procedure

Spent shale with the size 16 to 35 U.S. mesh, which had been obtained from the retorting process, was charged into the adsorption column, the column was connected to the system, was set to a desired temperature, and the column was immersed in the constant temperature bath. The inert N_2 gas was then passed through the system to flush out any impurities. The gas flow through the system was heated to the bath temperature by approximately 60 feet of tubing before entering the adsorption column, the ultra-violet detector and the recorder were switched to on and the system was left for a few hours to reach the steady state conditions. The flow rate was set with a control valve and its value was measured by a flowmeter. The flowmeter was calibrated with a soap bubble flowmeter.

The procedure which was used during the runs was as below:

- a) For making the span for each gas concentration:
 - 1) All valves should be closed (including valve B)
 - 2) Open valves F, C, and H
 - 3) The flow rate should be adjusted to a constant value when the N_2 gas is passing through the system with valves D and B

- 4) The U.V. cell detector should be set to zero
- 5) Valve A should be opened at the same time that valve C is closed. The pen on the recorder will be moved to a maximum displacement corresponding to the concentration of H₂S gas.
- 6) By changing the span on the recorder the height of the breakthrough curve will be changed.
- 7) Valve A should be closed and valve F should be opened and the system should be left for 15 minutes. Now the system is ready for injection of the sample gas.

b) The Sample injection:

- 1) Valves I and K should be opened
- 2) Valve H should be closed and the system not disturbed for 10 minutes
- 3) Valve A should be opened and at the same time valve F should be closed. Now the recorder will start to record a breakthrough curve.

RESULTS AND DISCUSSIONAdsorption

Shale samples were produced in the previously described retort and were analyzed for mineral composition by x-ray diffraction analyses. Since the starting composition (before heating) was the same for all samples. Observed differences in the x-ray patterns are a direct result of the heating. The most noticeable of these differences is due to decomposition of the carbonate minerals in the upper range of temperatures. By 650°C, the dolomite $[Ca Mg (CO_3)_2]$ has started to breakdown, with evolution of CO_2 and formation of Periclase (MgO). By 750°C, breakdown of the calcite ($CaCO_3 + \text{heat} \rightarrow CaO + CO_2 \uparrow$) and formation of lime (CaO) is also evident. By 950°C, all of the carbonates are gone and new silicates (melitite and pyroxene) are beginning to form at the expense of feldspar, quartz, and the oxides from the carbonates. The zeolite mineral, analcime, also appears to break down in the upper 100-200°C of heating. These results are given in Table (1).

Table 1

X-Ray Diffraction Analysis of Shale Samples Retorted for Two Hours *

Sample No. and Heating Temp.	Quartz (SiO ₂)	Alkali Feldspar (Na,K)AlSi ₃ O ₈	Dolomite [(Na,K)AlSi ₃ O ₈]	Calcite (CaCO ₃)	Periclase (MgO)	Lime (CaO)	Portlandite Ca(OH) ₂	Siderite (?) (FeCO ₃)	Muscovite KAl ₂ (AlSi ₃ O ₁₀)(OH) ₂	Analcime (NaAlSi ₂ O ₆ ·H ₂ O)
CSM-P-11 (250 C)	Major	Moderate	Major	Moderate				Minor	Trace	Moderate
CSM-P-22 (350 C)	Major	Moderate	Major	Moderate				Minor	Trace	Moderate
CSM-P-33 (450 C)	Major	Moderate	Major	Major-Moderate				Minor	Trace	Moderate
CSM-P-44 (550 C)	Major	Moderate	Major	Major-Moderate				Minor	Trace	Moderate
CSM-P-55 (650 C)	Major	Moderate	Major (but P-44)	Major-Moderate	Minor			Trace	Trace	Moderate
CSM-P-66 (750 C)	Major	Moderate	Moderate (P-55)	Major-Moderate	Minor-Moderate (P-55)				Trace	Moderate Minor (P-55)
CSM-P-77 (850 C)	Major	Moderate-Major	Minor (P-66)	Minor (P-66)	Moderate (P-66)	Minor				Minor-Trace (P-66)
CSM-P-88 (950 C)	Major-Moderate (P-77)	Moderate (P-77)			Moderate (P-77)	Minor				Trace? (P-77)

Major = 30%
 Moderate = 10-30%
 Minor = 3-10%
 Trace = %

* This analysis was made by the CSM Research Institute.

The BET surface areas of the oil shale retorted at different temperatures ranging from 350 to 950°C were obtained and these results are given in Table (2) and Figure (5). As indicated in Table (2). (The sample calculations are given in Appendix I.)

Table 2

The BET Surface Area of Oil Shale Retorted for Two Hours

<u>Temperature °</u>	<u>BET Surface Area (m²/gm)</u>
350	0.4
450	1.5
550	4.3
650	6.4
750	8.8
950	6.9

A chemical analysis of the retorted oil shale was also obtained, and these results are given in Table (3). It may be seen from Table (3), that the total residual carbon decreases with increasing retorting temperature.

A comparison was made of adsorption capacities measured under similar experimental conditions but using samples of the spent shale that had been retorted at temperatures ranging from 350 to 950 °C in 100 C intervals. The results of this experiment are shown in Table 4 and Figure (6). As can be seen in Figure (6), the equilibrium uptake of H₂S on the spent shale is a function of retorting temperature.

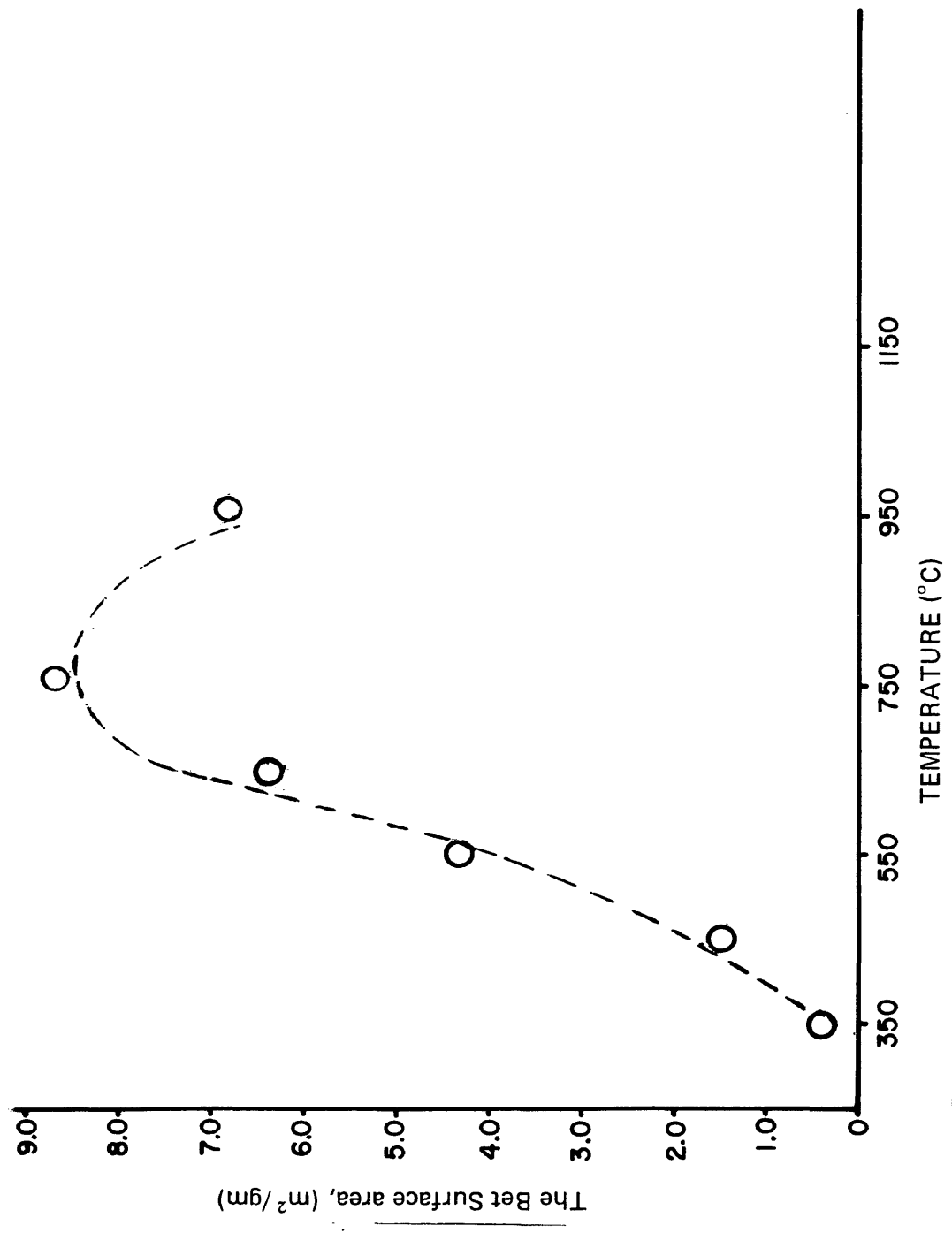


FIGURE 5. THE BET SURFACE AREA OF THE SPENT SHALE RETORTED FOR TWO HOURS AT DIFFERENT TEMPERATURES RANGING FROM 350 TO 950°C

Table 3

Chemical Analyses of Oil Shale Retorted for Two Hours*

Retorting Temperature, °C	Weight Percent							Heat Content, Btu
	Carbon	Hydrogen	Nitrogen	Sulfur	Others Minerals	Mineral Carbon	Organic Carbon	
250	18.89	2.05	0.68	0.61	77.77	4.40	14.49	3,831
350	19.96	2.32	0.72	0.65	76.35	4.37	15.59	4,119
450	12.51	0.83	0.60	0.55	85.51	4.98	7.53	2,252
550	10.26	0.18	0.45	0.49	88.62	4.99	5.27	1,580
650	9.27	0.17	0.41	0.50	89.65	4.41	4.86	1,424
750	8.77	0.12	0.37	0.54	90.74	3.72	5.05	1,325
850	6.63	0.21	0.24	0.70	92.22	1.62	5.01	1,050
950	4.79	0.14	0.13	0.69	94.25	.62	4.17	733

* Chemical analysis was made at the Larmie Energy Research Center.

Table 4

Adsorption of H₂S on Spent Shale at 7 °C Using a
Concentration of 10,000 ppm H₂S in Nitrogen gas

<u>Retorting Temperature C</u>	<u>Area under breakthrough curve, (in²)</u>	<u>cm³ H₂S gm solid</u>	<u>q*, mgm H₂S gm solid</u>
350	2.34	0.37397	0.519
	2.13	0.35675	
	<u>2.24</u>	<u>0.36536</u>	
450	6.08	1.00690	1.618
	7.59	1.27256	
	<u>6.84</u>	<u>1.13973</u>	
550	9.47	1.62836	2.429
	10.43	1.79252	
	<u>9.95</u>	<u>1.71044</u>	
650	10.97	1.81599	2.647
	11.43	2.00331	
	10.23	1.66212	
	12.16	1.97626	
	<u>11.20</u>	<u>1.86442</u>	
750	11.63	1.88962	2.969
	13.13	2.20136	
	12.13	2.03350	
	12.30	2.11248	
	14.16	2.30171	
	10.20	1.66851	
	14.95	2.42996	
	<u>12.64</u>	<u>2.42996</u>	
950	11.36	1.83579	2.424
	10.64	1.72882	
	8.73	1.41955	
	11.34	1.84358	
	<u>10.52</u>	<u>1.70692</u>	

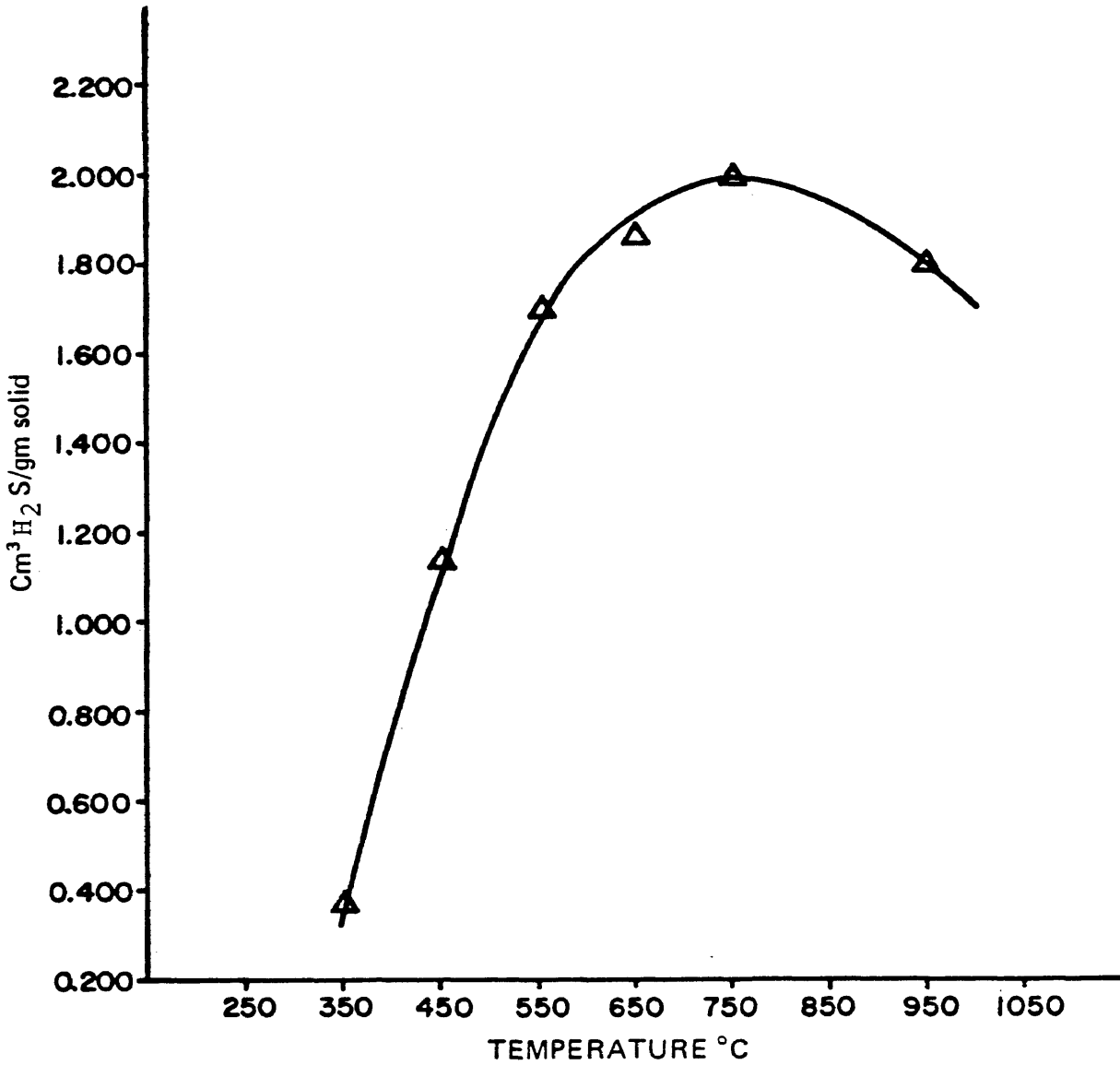


FIGURE 6. ADSORPTION AT 7°C OF H₂S ON SPENT SHALE AT 7°C FOR SHALE RETORTED AT TEMPERATURES RANGING FROM 350 TO 950°C.

The maximum uptake of H₂S took place on shale that had been retorted in the temperature interval between 650 and 750°C. The highest uptake was at 750°C. This may be attributed to changes in the structure of the shale that results from the reaction of calcite and dolomite. Although the uptake of H₂S was expected to decrease with decreasing residual carbon, this was not found.

Because the maximum H₂S uptake occurred on samples that had been retorted between 650 and 750°C, shale retorted at 750 C was selected for further adsorption studies and experimental breakthrough curves were obtained at 10, 25, and 60 C for concentrations of 1000, 2000, 3000, 5000, 7000 and 10,000 ppm H₂S in dry nitrogen gas. This was done in a packed bed of spent shale about 6 inches long with the particle sizes ranging from 16 to 35 U.S. mesh. The gas flow rate was set at 67.04 (cm³/min.). Typical experimental sorption curves are shown in the Figures (7), (8), and (9). The actual data for experimental breakthrough curves are shown in Appendix IX with all necessary information for calculations. Replicate runs were necessary because of the non-homogeneous nature of the spent shale, therefore, the average of those runs were used to plot the curves. These show the effect of adsorbate concentration on the breakpoint.

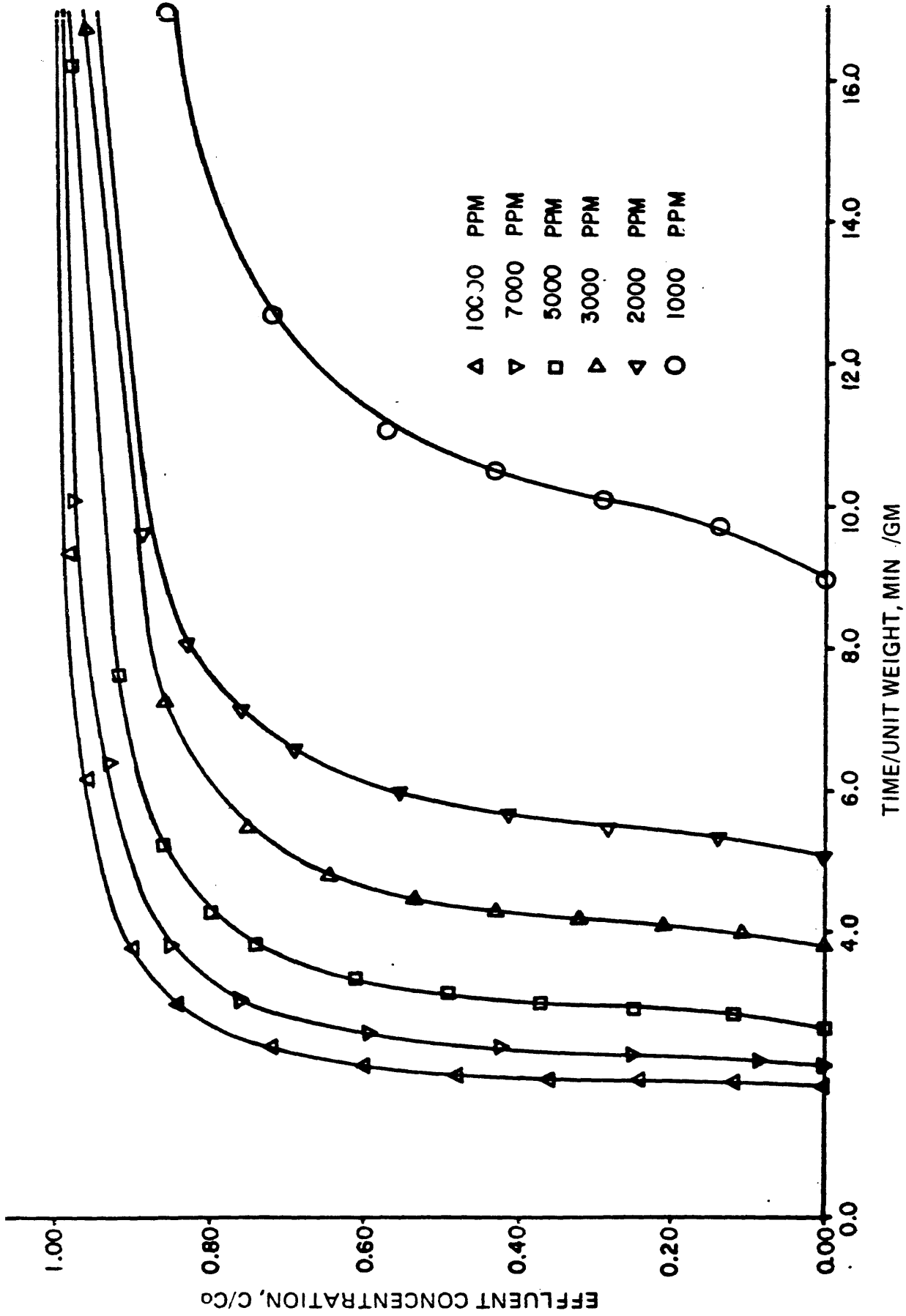


FIGURE 7. COMPARISON OF EXPERIMENTAL BREAKTHROUGH CURVE FOR CONCENTRATIONS OF 1000, 2000, 3000, 5000, AND 10,000 PPM H₂S IN NITROGEN AT 10°C.

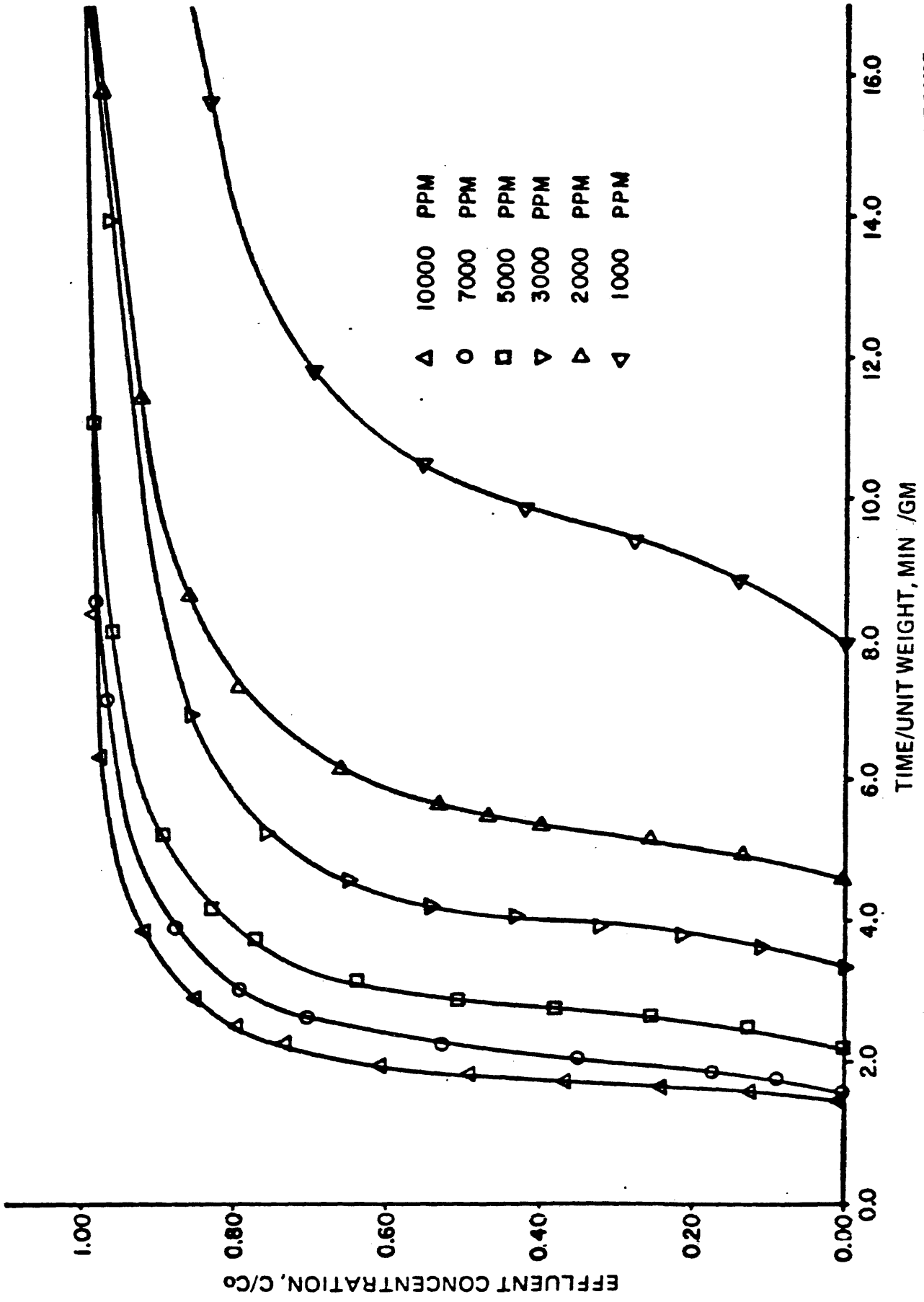


FIGURE 8. COMPARISON OF EXPERIMENTAL BREAKTHROUGH CURVES FOR CONCENTRATIONS OF 1000, 2000, 3000, 5000, 7000, 10,000 PPM H₂S IN NITROGEN AT 25°C.

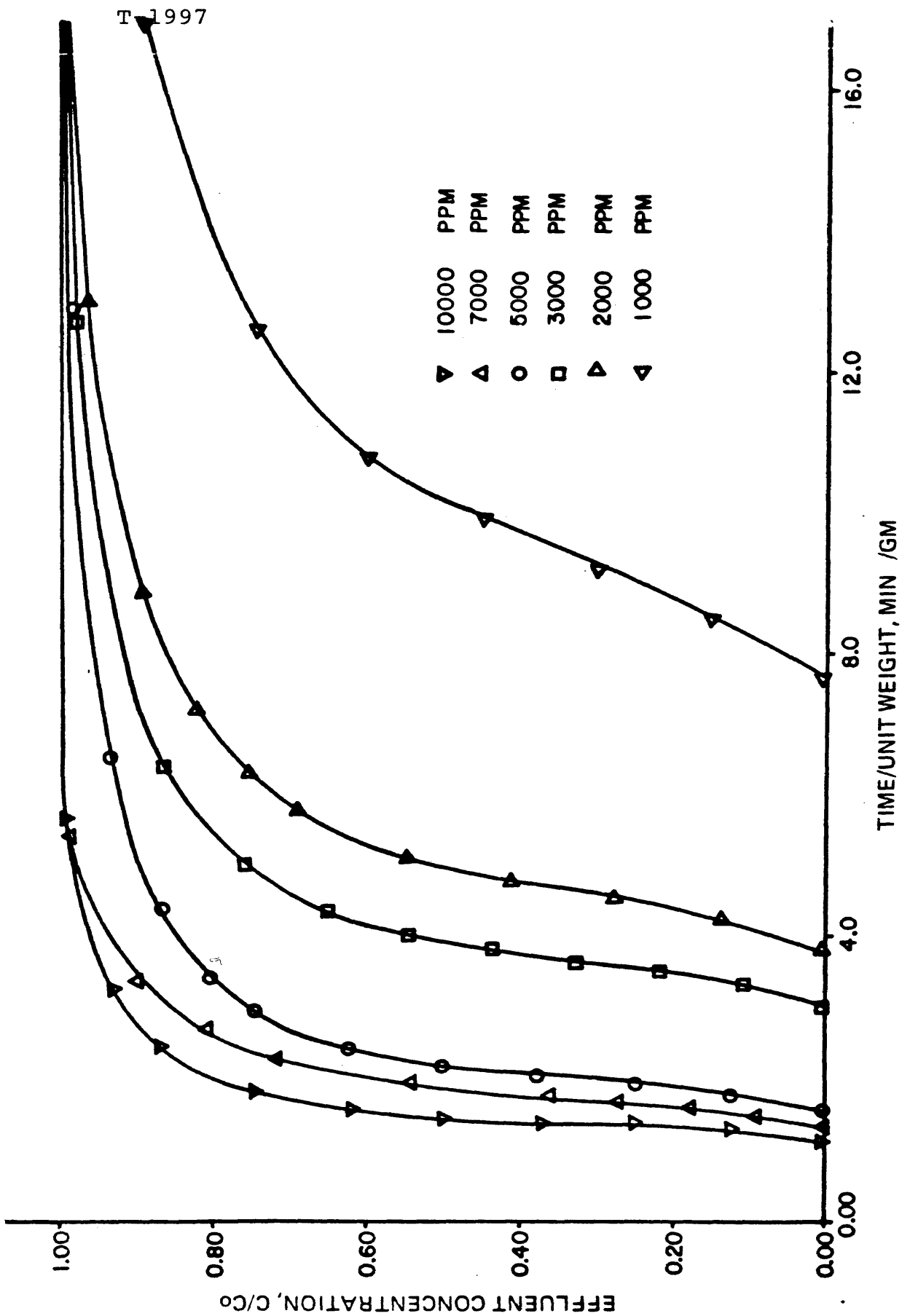


FIGURE 9. COMPARISON OF EXPERIMENTAL BREAKTHROUGH CURVES FOR CONCENTRATIONS OF 1000, 2000, 3000, 5000, 7000, and 10,000 PPM H₂S IN NITROGEN AT 60°C.

Also, a comparison between the sorption curves for each concentration are shown in Figures (10), (11), (12), (13), (14), and (15) at the temperatures 10, 25, and 60°C. As expected, the time required to reach the breakpoint increased as the temperature decreased.

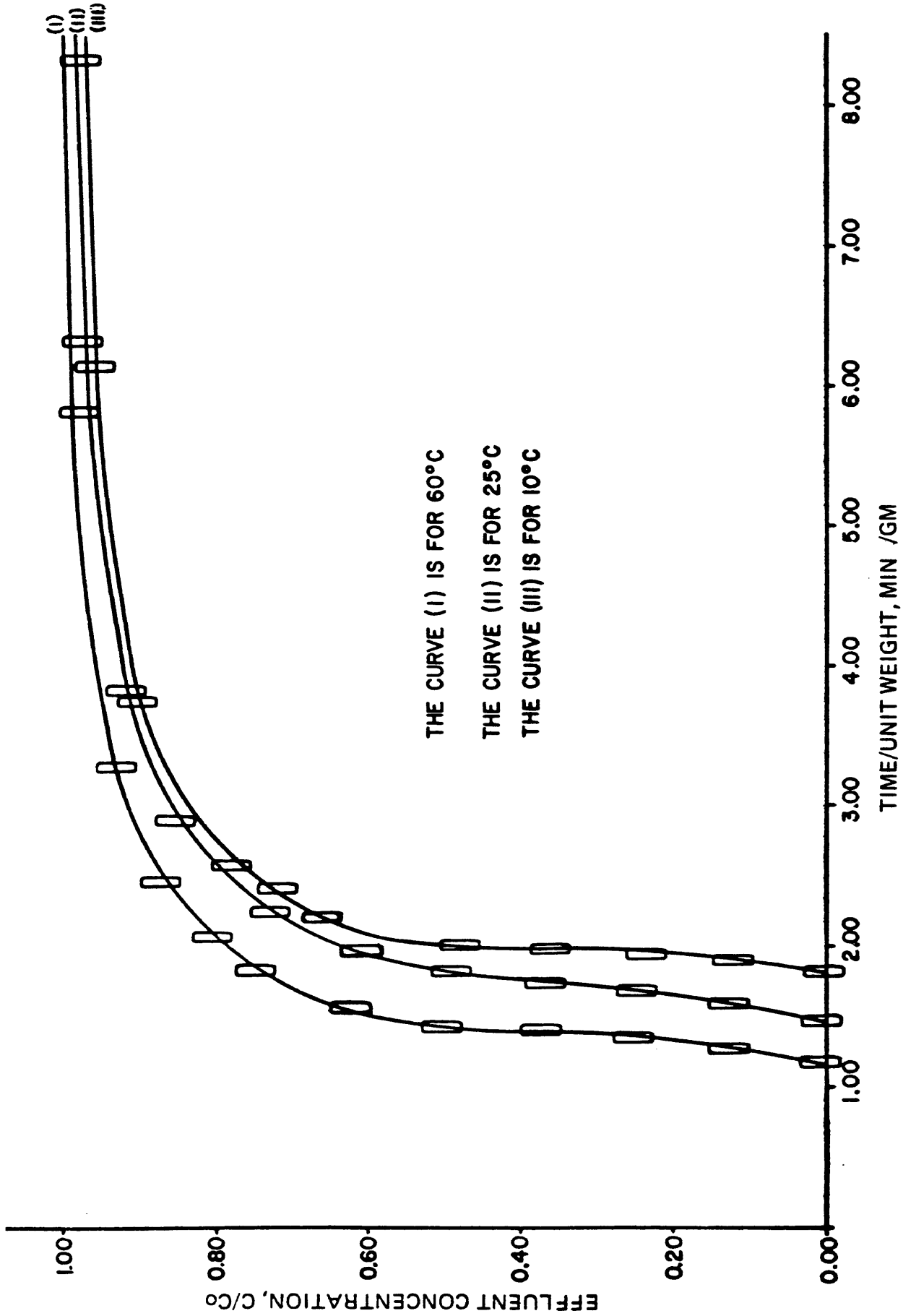


FIGURE 10. COMPARISON OF BREAKTHROUGH CURVES FOR THE CONCENTRATION 10,000 PPM H₂S IN NITROGEN AT 10°C, 25°C, AND 60°C.

T-1997

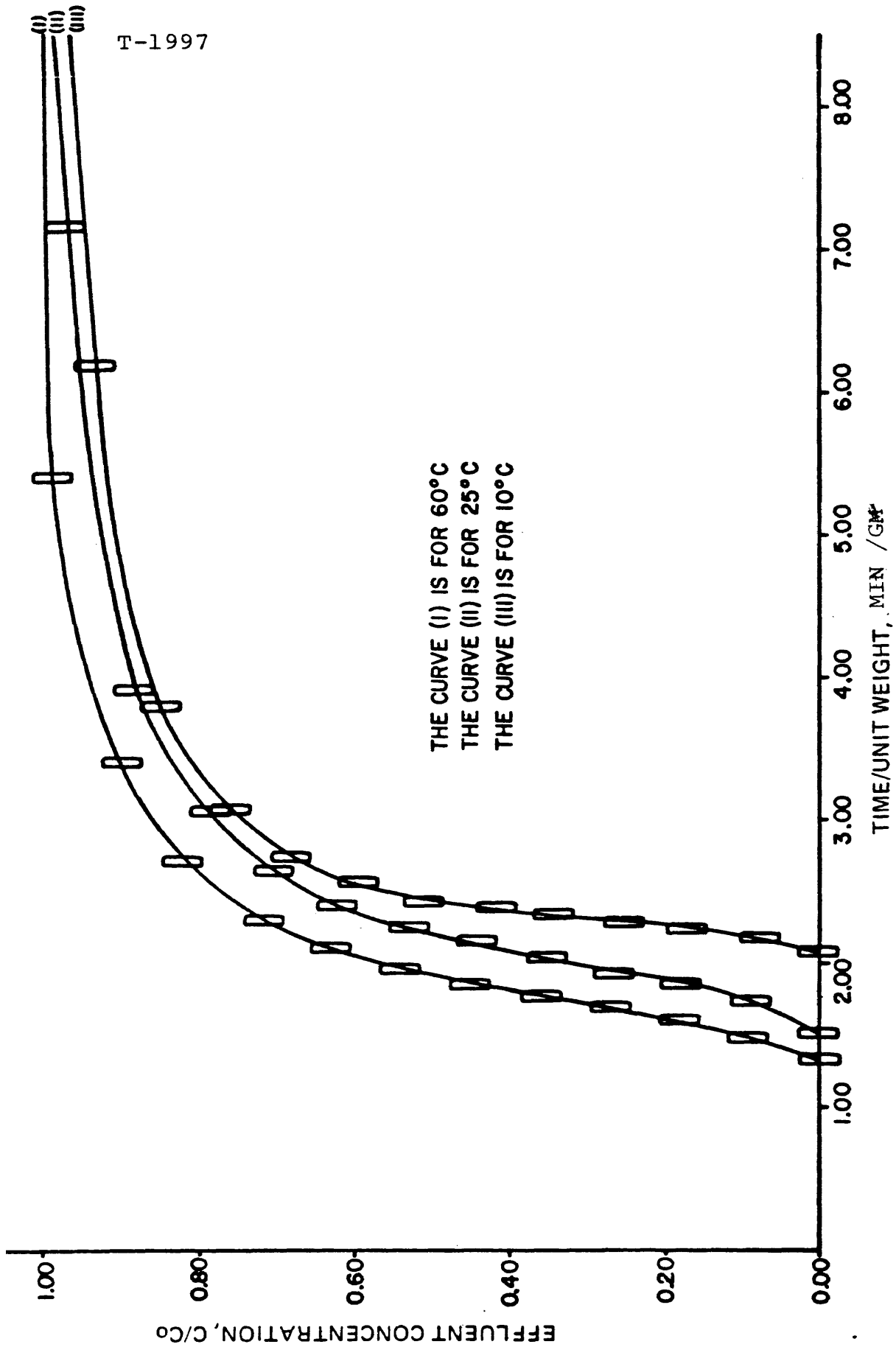


FIGURE 11. COMPARISON OF BREAKTHROUGH CURVES FOR THE CONCENTRATION 7000 PPM H₂S IN NITROGEN AT 10°C, 25°C, AND 60°C.

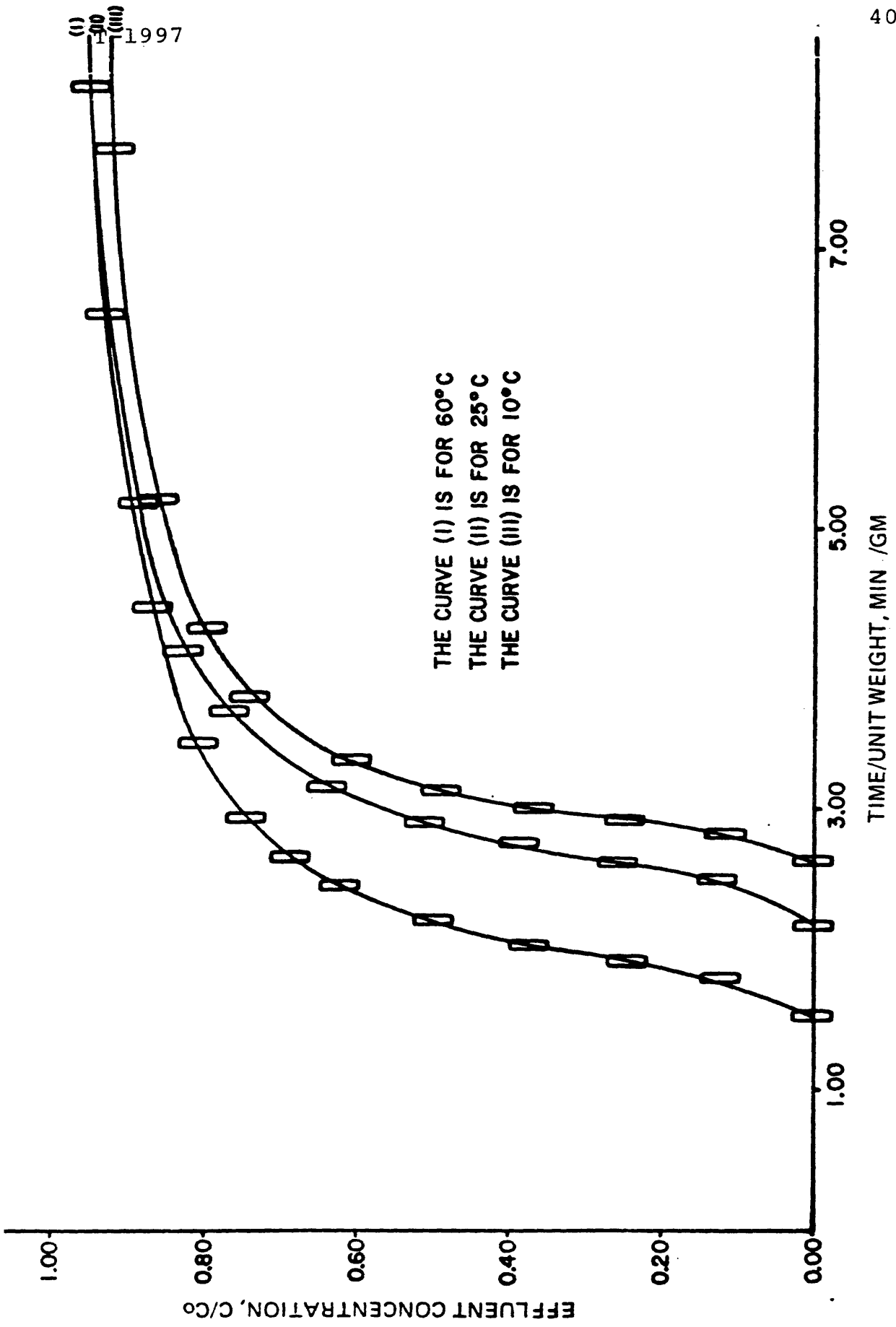


FIGURE 12. COMPARISON OF BREAKTHROUGH CURVES FOR THE CONCENTRATION 5000 PPM H₂S IN NITROGEN AT 10°C, 25°C, AND 60°C.

T-1997

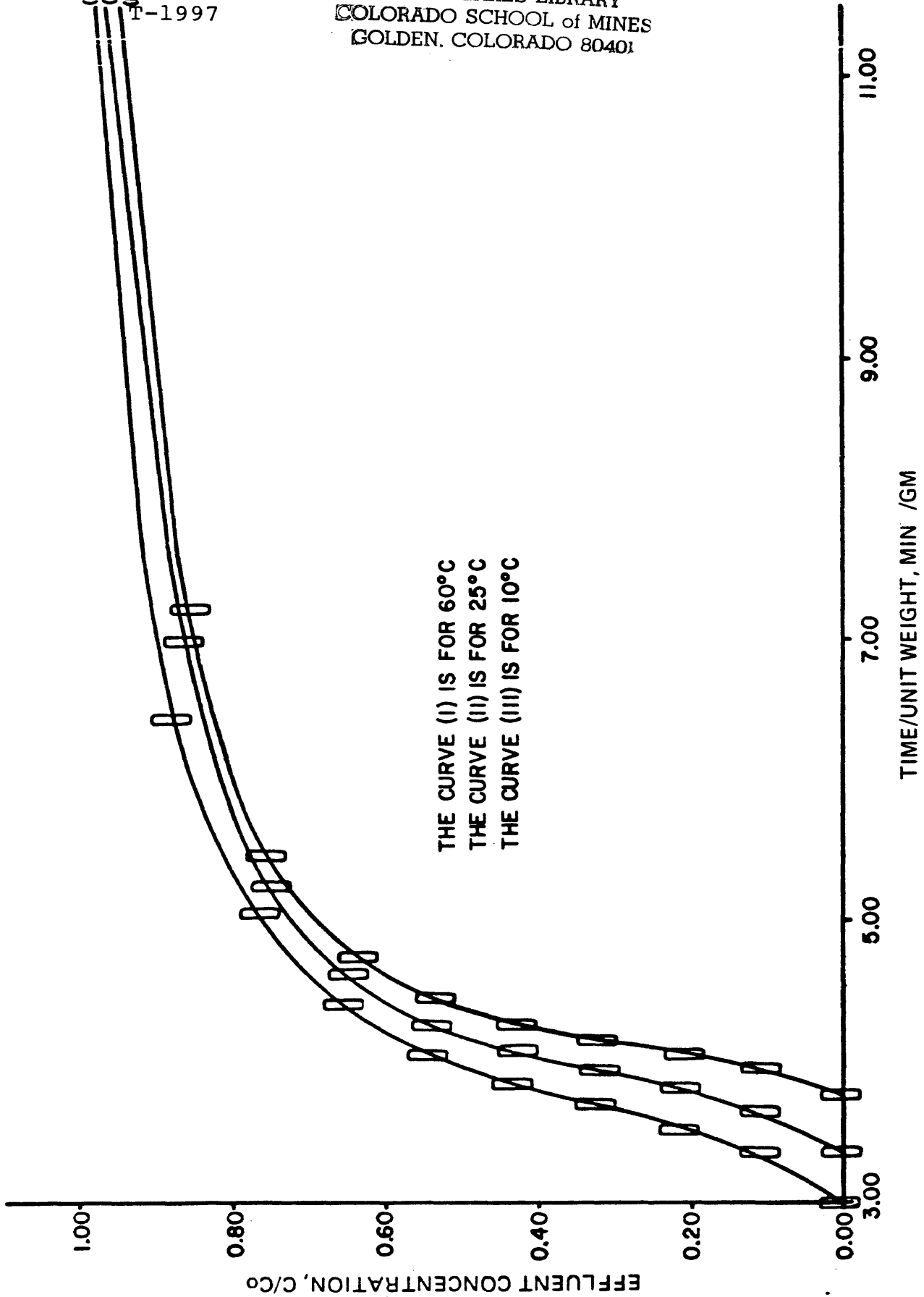


FIGURE 13. COMPARISON OF BREAKTHROUGH CURVES FOR THE CONCENTRATION 3000 PPM H₂S IN NITROGEN AT 10°C, 25°C, AND 60°C.

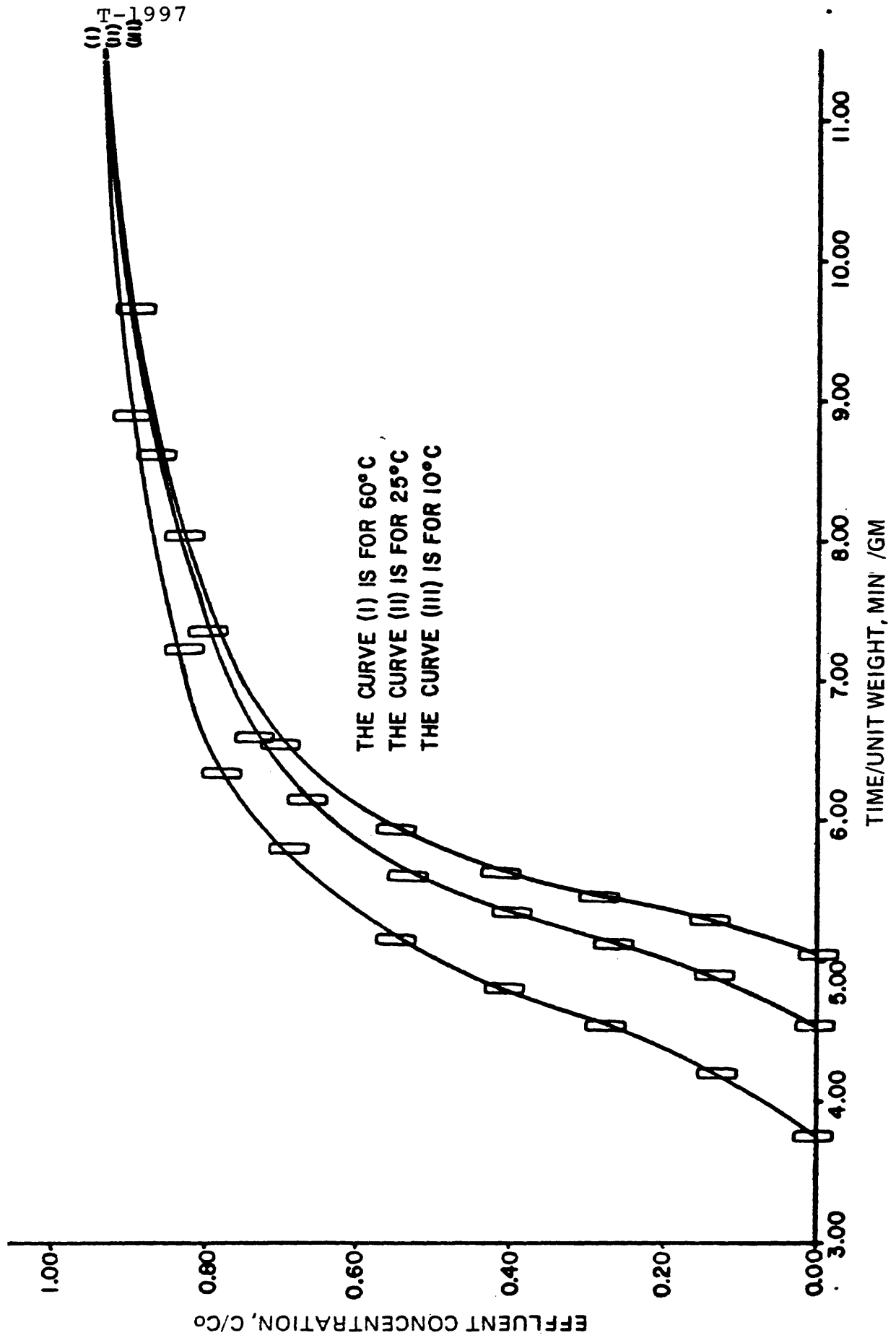


FIGURE 14. COMPARISON OF BREAKTHROUGH CURVES FOR THE CONCENTRATION 2000 PPM H₂S IN NITROGEN AT 10°C, 25°C, and 60°C.

(I) T-1997
(II)
(III)

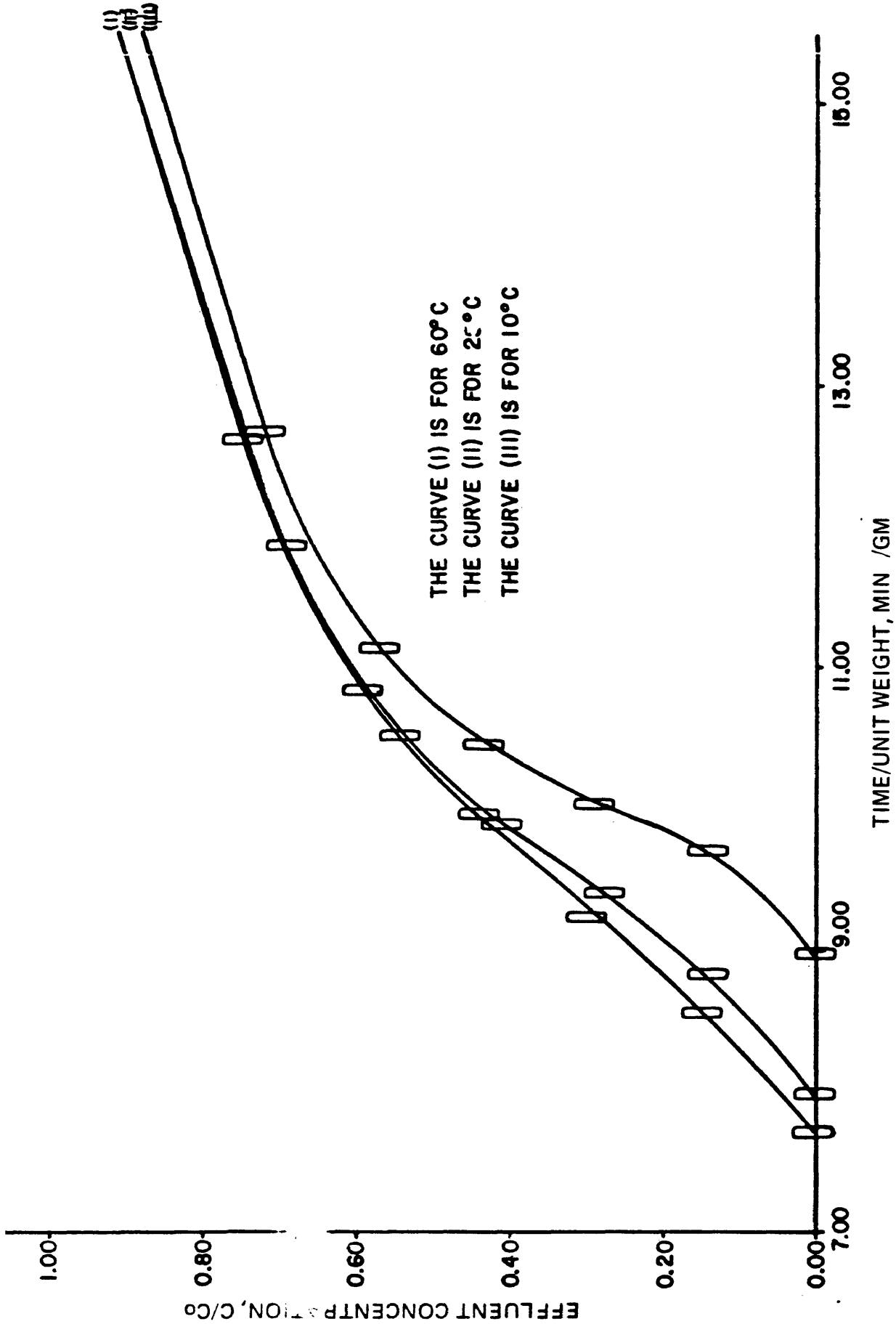


FIGURE 15. COMPARISON OF BREAKTHROUGH CURVES FOR THE CONCENTRATION 1000 PPM H₂S IN NITROGEN AT 10°C, 25°C, AND 60°C.

For each run the area under the breakthrough curve was measured with a polar planimeters and the concentration of adsorbate gas on spent shale was calculated (the sample calculations are given in Appendix VI) for each temperature. The equilibrium isotherm data and the Langmuir constant are shown in Table 5. The plot of the amount of adsorbed gas versus concentration is called equilibrium isotherms. These isotherms are shown in Figures (16) and (20), and the necessary data are given in Tables 6, 7, and 8. Replicate runs were necessary because of the non-homogeneous nature of the spent shale. Therefore, the average of those runs were obtained in this calculation for the similar experimental condition and concentration. The equilibrium isotherms in Figures (16) and (20) were fit accurately with the type one isotherms which were discussed before and this type was proposed by Freundlich and Langmuir.

T-1997

Table 5

Equilibrium Isotherm Data and Langmuir Constants, for
H₂S on Spent Shale,

$$q^* = \frac{Q_0 C^*}{1 + Q_1 C^*}$$

C	C*, gm H ₂ S	q*, gm. H ₂ S	Q ₀	Q ₁ , cm ³	Q ₁ C ₀
	cm ³ total gas	cm ³ solid		gm H ₂ S	
10	0.00000142	0.00188	2245.0066	5.66856x10 ⁵	0.79
	0.00000284	0.00210	"	"	1.61
	0.00000426	0.00264	"	"	2.42
	0.00000711	0.00324	"	"	4.03
	0.00000995	0.00357	"	"	5.64
	0.00001422	0.00396	"	"	8.06
25	0.00000143	0.00188	2760.512	8.55563x10 ⁵	1.22
	0.00000286	0.00200	"	"	2.45
	0.00000429	0.00241	"	"	3.67
	0.00000715	0.00274	"	"	6.12
	0.00001001	0.00294	"	"	8.56
	0.00001429	0.00345	"	"	12.22
60	0.00000145	0.00181	3237.5347	11.94660x10 ⁵	1.73
	0.00000289	0.00187	"	"	3.45
	0.00000434	0.00222	"	"	5.18
	0.00000723	0.00236	"	"	8.63
	0.00001013	0.00245	"	"	12.10
	0.00001447	0.00299	"	"	17.29

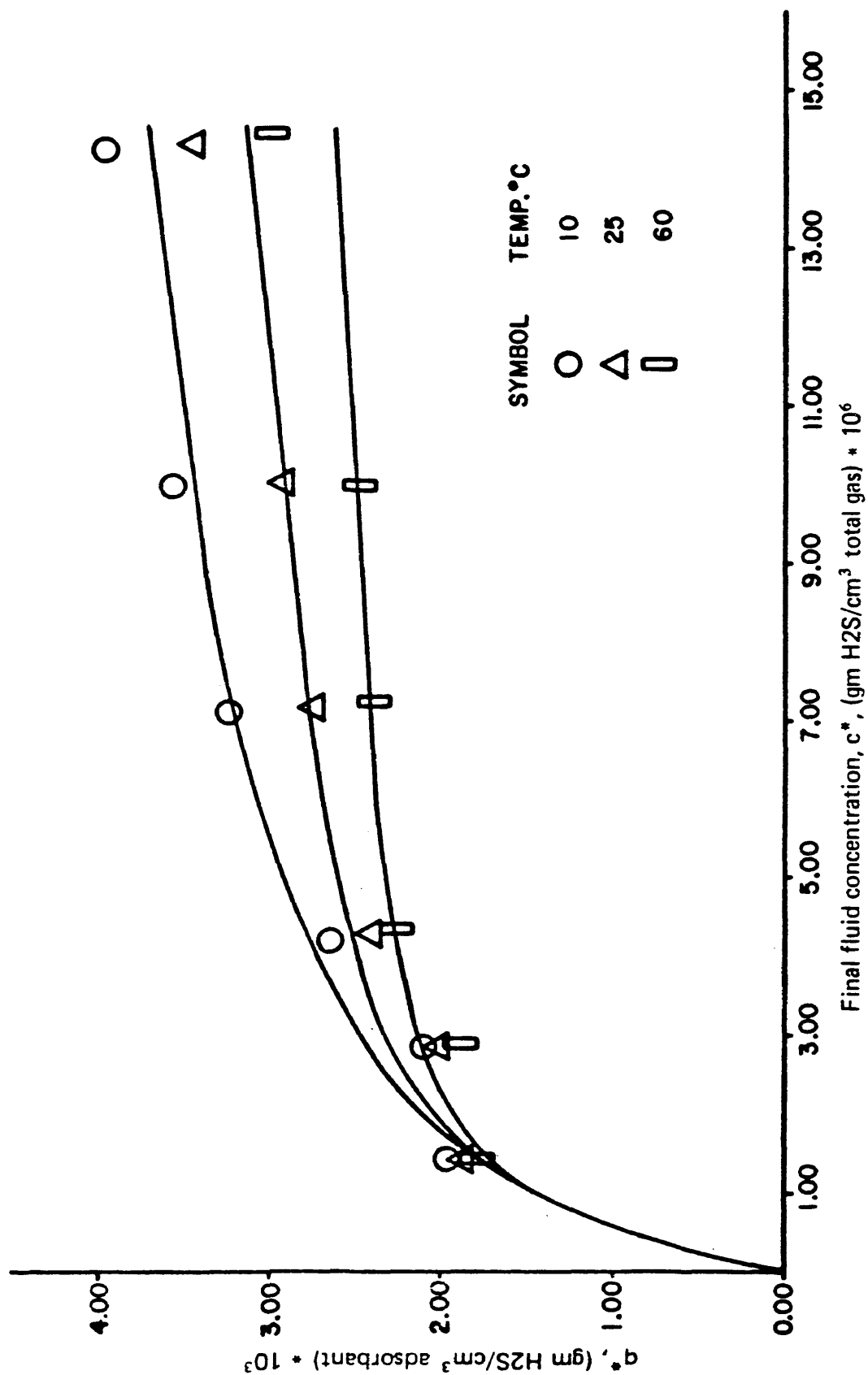


FIGURE 16. EQUILIBRIUM ISOTHERMS FOR ADSORPTION OF H₂S ON SPENT SHALE AT 10°C, 25°C, and 60°C FIT TO THE LANGMUIR EQUATION.

Table 6

Equilibrium Adsorption Quantities of H₂S at 10°C

on the Spent Shale Retorted at 750°C

Concentration H ₂ S in N ₂ PPM, C*	Concentration H ₂ S in N ₂ , C* gm H ₂ S cm ³ Total gas		Equilibrium uptake, (q*) cm ³ H ₂ S/gm solid			Avg. Value cm ³ H ₂ S gm solid	q* gm. H ₂ S cm ³ solid
	Run #1	Run #2	Run #3	Run #1	Run #2		
1000	0.000001421	0.79232	0.77943	0.94357	0.83844	0.00188	
2000	0.000002843	0.89240	0.98818	0.92930	0.93663	0.00210	
3000	0.000004648	1.15274	1.11192	1.25565	1.17344	0.00264	
5000	0.00000711	1.36502	1.50464	1.46324	1.44430	0.00324	
7000	0.000009950	1.51197	1.55419	1.46291	1.50969	0.00357	
10,000	0.000014220	1.81163	1.77125	1.70031	1.76106	0.00396	

Table 7

Equilibrium Adsorption Quantities of H₂S at 25°C

on the Spent Shale Retorted at 750°C

Concentration H ₂ S in N ₂ PPM. C*	Concentration H ₂ S in N ₂ , C*		Equilibrium uptake q*			Avg. Value	q*
	$\frac{\text{gm H}_2\text{S}}{\text{cm}^3 \text{ Total gas}}$	$\frac{\text{cm}^3 \text{H}_2\text{S}}{\text{gm solid}}$	Run #1	Run #2	Run #3	$\frac{\text{cm}^3 \text{H}_2\text{S}}{\text{gm solid}}$	$\frac{\text{gm H}_2\text{S}}{\text{cm}^3 \text{ solid}}$
1000	0.00000143	0.86047	0.83071	0.85016	0.84711	0.84711	0.0018845
2000	0.00000286	0.91587	0.82615	0.92255	0.88819	0.88819	0.0020060
3000	0.00000409	1.11505	1.00762	0.08884	1.07050	1.07050	0.0024176
5000	0.00000715	1.26160	1.24272	1.14163	1.21532	1.21532	0.0027447
7000	0.00001001	1.33121	1.28903	1.28974	1.30332	1.30332	0.0029435
10,000	0.00001429	1.67750	1.36155	1.55110	1.53005	1.53005	0.0034555

Table 8

Equilibrium Adsorption Quantities of H₂S at 60°C

on the Spent Shale Retorted at 750°C

Concentration H ₂ S in N ₂ PPM	Concentration H ₂ S in N ₂ , C* gm H ₂ S	Equilibrium Uptake, q*				Run #4	Avg. value, cm ³ H ₂ S gm solid	q* gm. H ₂ S cc. solid
		cm ³ total gas	Run #1	Run #2	Run #3			
1000	0.00000145	0.7932	0.7558	0.8262	--	0.7917	0.00180958	
2000	0.00000289	0.8403	0.7711	0.7506	0.9235	0.8213	0.00187738	
3000	0.00000434	0.9673	1.1213	0.8309	--	0.9732	0.00222459	
5000	0.00000723	0.9916	0.9306	1.1796	--	1.0340	0.00236347	
7000	0.00001013	0.9898	0.9950	1.2338	--	1.0729	0.00245245	
10,000	0.00001422	1.4930	1.3002	1.3763	1.0701	1.3099	0.00299409	

Using the values given in Tables 6, 7, and 8, the equations for a Langmuir isotherm were obtained from a least squares analysis, (the details of the computer program which was used for this type of isotherm are given in Appendix II) and are given below for different temperatures:

$$q^* = \frac{(2.2450066 \times 10^3) C^*}{1 + (5.6685626 \times 10^5) C^*} \quad \text{for } 10^\circ\text{C} \quad \text{Eq. (33)}$$

$$q^* = \frac{(2.7605120 \times 10^3) C^*}{1 + (8.5556316 \times 10^5) C^*} \quad \text{for } 25^\circ\text{C} \quad \text{Eq. (34)}$$

$$q^* = \frac{(3.2375347 \times 10^3) C^*}{1 + (1.1946460 \times 10^6) C^*} \quad \text{for } 60^\circ\text{C} \quad \text{Eq. (35)}$$

The value C^* is the gas concentration of H_2S in nitrogen, $(\frac{\text{gm H}_2\text{S}}{\text{Cm}^3 \text{ total gas}})$. The goodness of fit of the equation is demonstrated in Figure (17) for 10°C , in Figure (18) for 25°C , and in Figure (19) for 60°C . As can be seen from Figure (16), the data points were fit accurately with the Langmuir equation for all of the equilibrium isotherms.

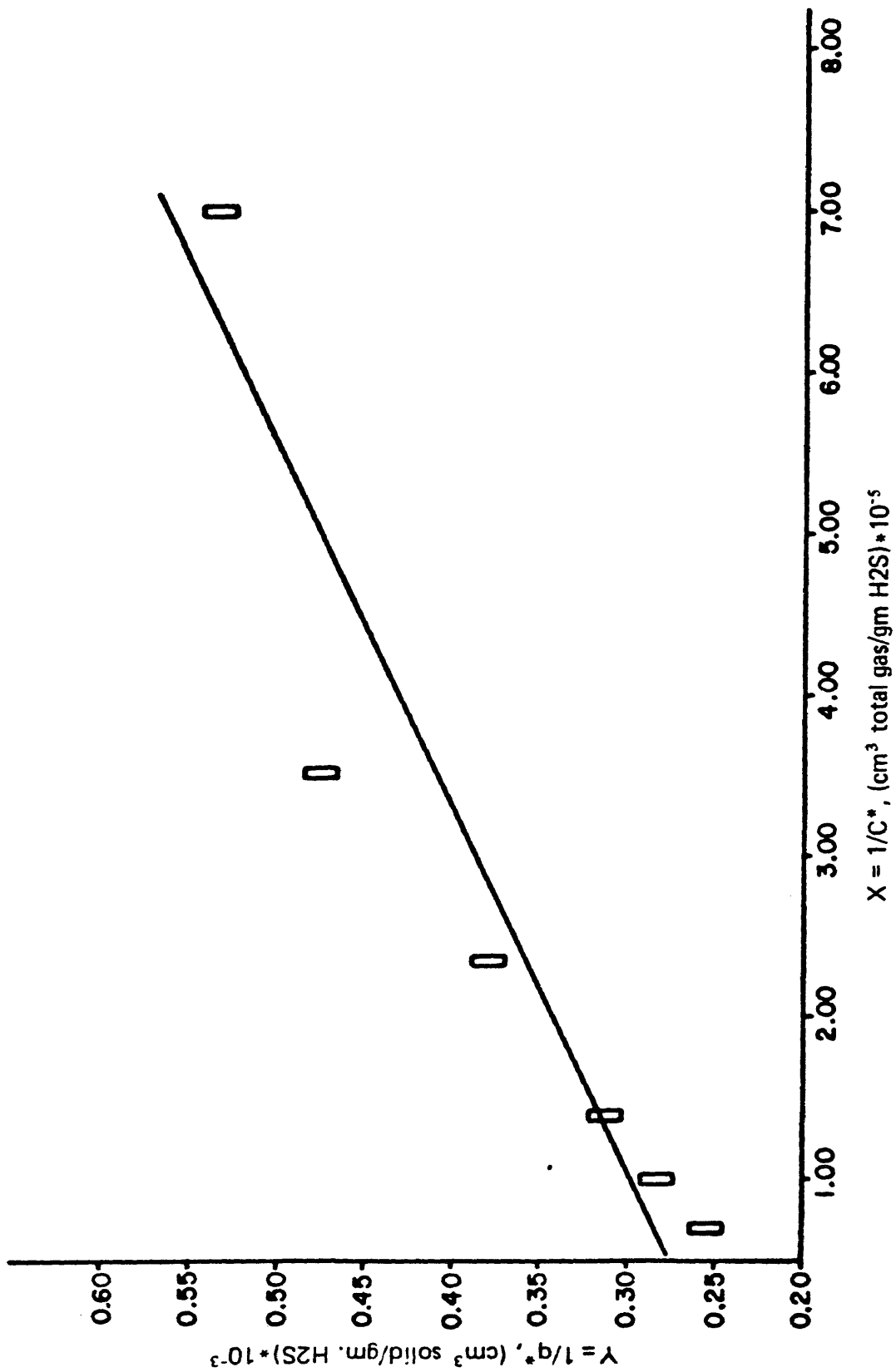


FIGURE 17. ADSORPTION ISOTHERMS OF H₂S ON SPENT SHALE AT 10°C PLOTTED ACCORDING TO THE LANGMUIR EQUATION² (TESTING OF THE LANGMUIR EQUATION).

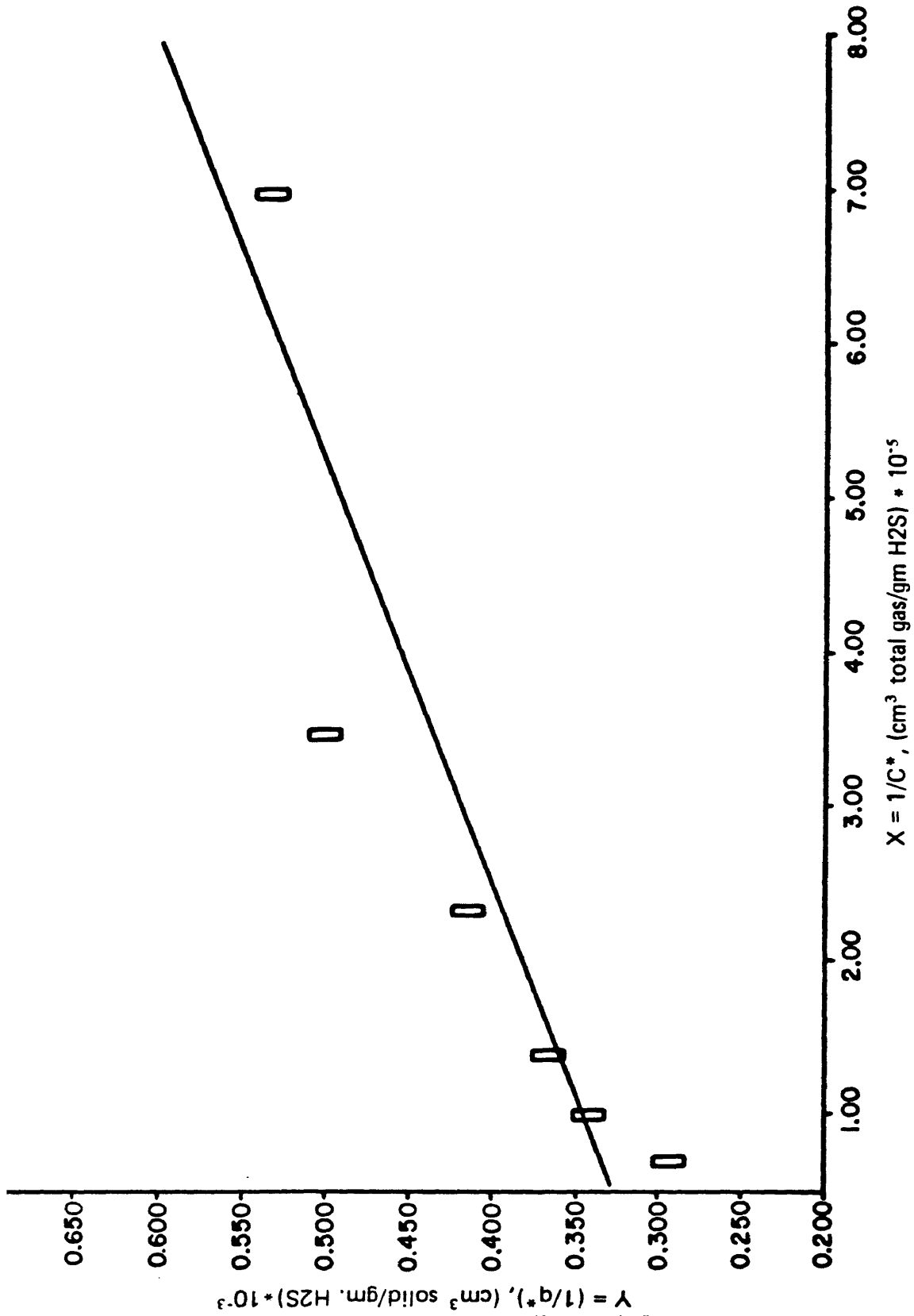


FIGURE 18. ADSORPTION ISOTHERMS OF H₂S ON SPENT SHALE AT 25°C PLOTTED ACCORDING TO THE LANGMUIR EQUATION (TESTING OF THE LANGMUIR EQUATION).

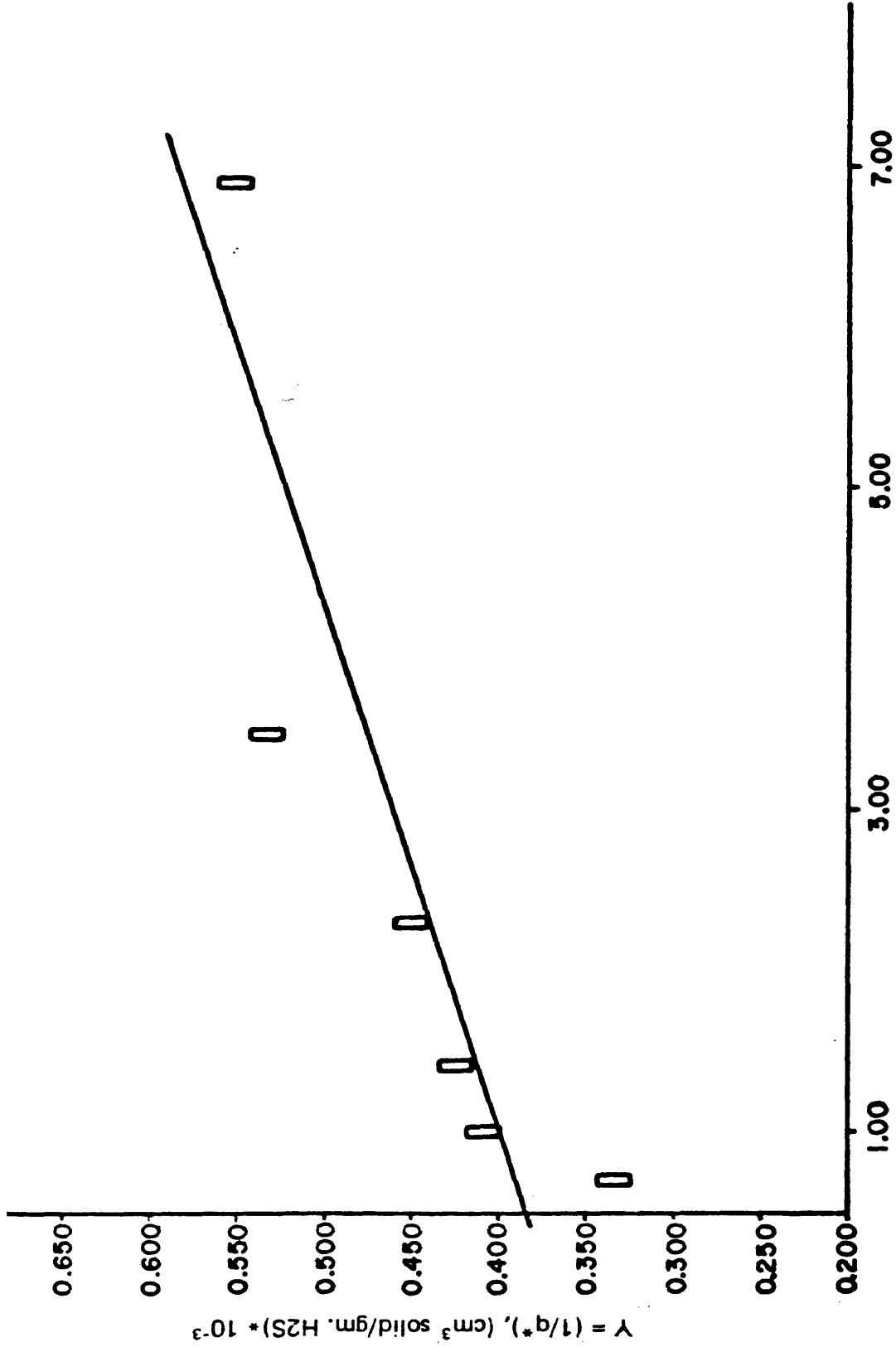


FIGURE 19. ADSORPTION ISOTHERMS OF H₂S ON SPENT SHALES AT 60°C PLOTTED ACCORDING TO THE LANGMUIR EQUATION (TESTING OF THE LANGMUIR EQUATION).

In the same manner, using the values given in Tables 5, 6, and 7, the equation for a Freundlich isotherm were obtained from a least squares analysis (the details of the computer program which was used for this type of isotherm are given in Appendix III) and are given below for different temperatures:

$$q^* = (0.1918605) (C^*)^{(0.3469361)} \quad \text{for } 10^\circ\text{C} \quad \text{Eq. (36)}$$

$$q^* = (0.0658124) (C^*)^{(0.26788929)} \quad \text{for } 25^\circ\text{C} \quad \text{Eq. (37)}$$

$$q^* = (0.0285254) (C^*)^{(0.20853133)} \quad \text{for } 60^\circ\text{C} \quad \text{Eq. (38)}$$

The equilibrium isotherm data and the Freundlich constants are presented in Table 9 and the isotherms are plotted in Figure (20), according to Freundlich equation, $q^* = m (C^*)^{1/n}$.

The goodness of fit of the equation is demonstrated in Figure (21) for 10°C , in Figure (22) for 25°C , and in Figure (23) for 60°C . As can be seen from Fig. (20), the data points were also fit accurately with the Freundlich equation for all equilibrium isotherms.

Table 9

Equilibrium Isotherm Data and Freundlich Constants

Temp. °C	C^* , $\frac{\text{gm H}_2\text{S}}{\text{cm}^3 \text{ total gas}}$	q^* $\frac{\text{gm} \cdot \text{H}_2\text{S}}{\text{cm}^3 \text{ solid}}$	m	$1/n$
10 °C	0.00000142	0.00188	0.191860	0.34693618
	0.00000284	0.00210		
	0.00000426	0.00264		
	0.00000711	0.00324		
	0.00000995	0.00357		
	0.00001422	0.00396		
25 °C	0.00000143	0.00188	0.065848	0.26788929
	0.00000286	0.00200		
	0.00000429	0.00241		
	0.00000715	0.00274		
	0.00001001	0.00294		
	0.00001429	0.00345		
60 °C	0.00001450	0.00180	0.028544	0.20853133
	0.00000289	0.00187		
	0.00000434	0.00222		
	0.00000723	0.00236		
	0.00001013	0.00245		
	0.00001447	0.00299		

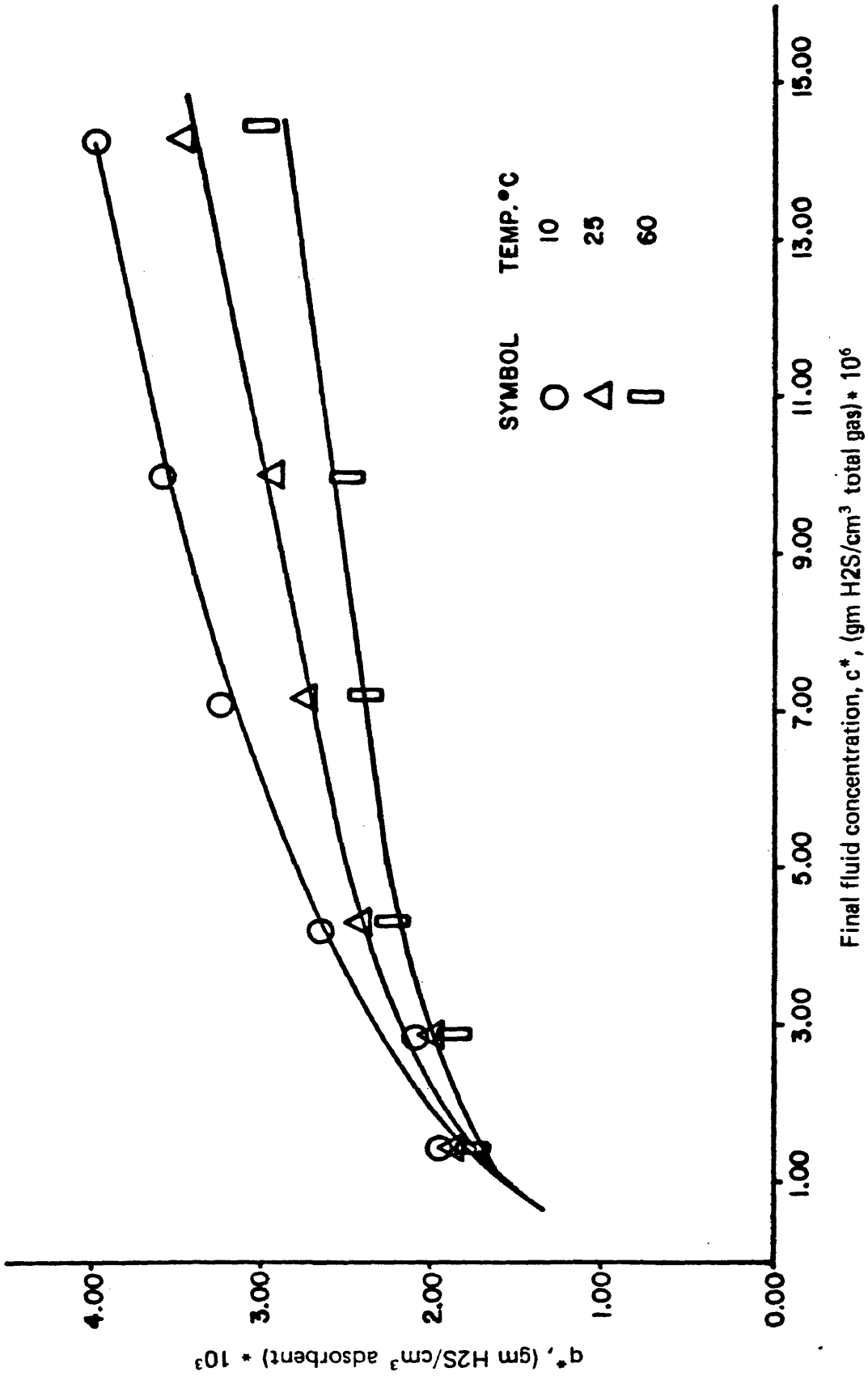


FIGURE 20. EQUILIBRIUM ISOTHERMS FOR ADSORPTION OF H_2S ON SPENT SHALE AT 10°C, 25°C, AND 60°C FIT TO THE FREUNDLICH EQUATION.

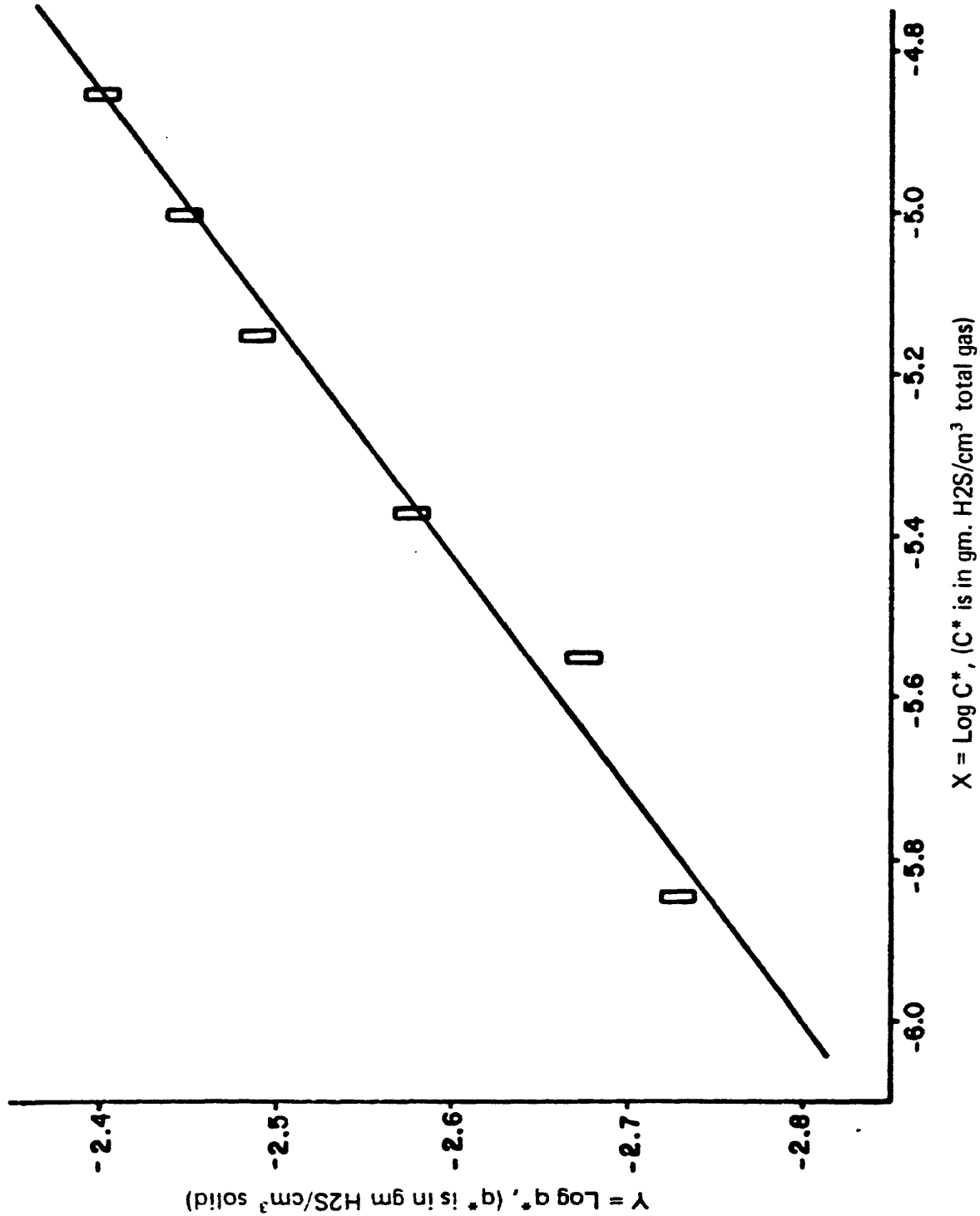


FIGURE 21. ADSORPTION ISOTHERMS OF H₂S ON SPENT SHALE AT 10°C PLOTTED ACCORDING TO THE FREUNDLICH EQUATION (TESTING OF THE FREUNDLICH EQUATION).

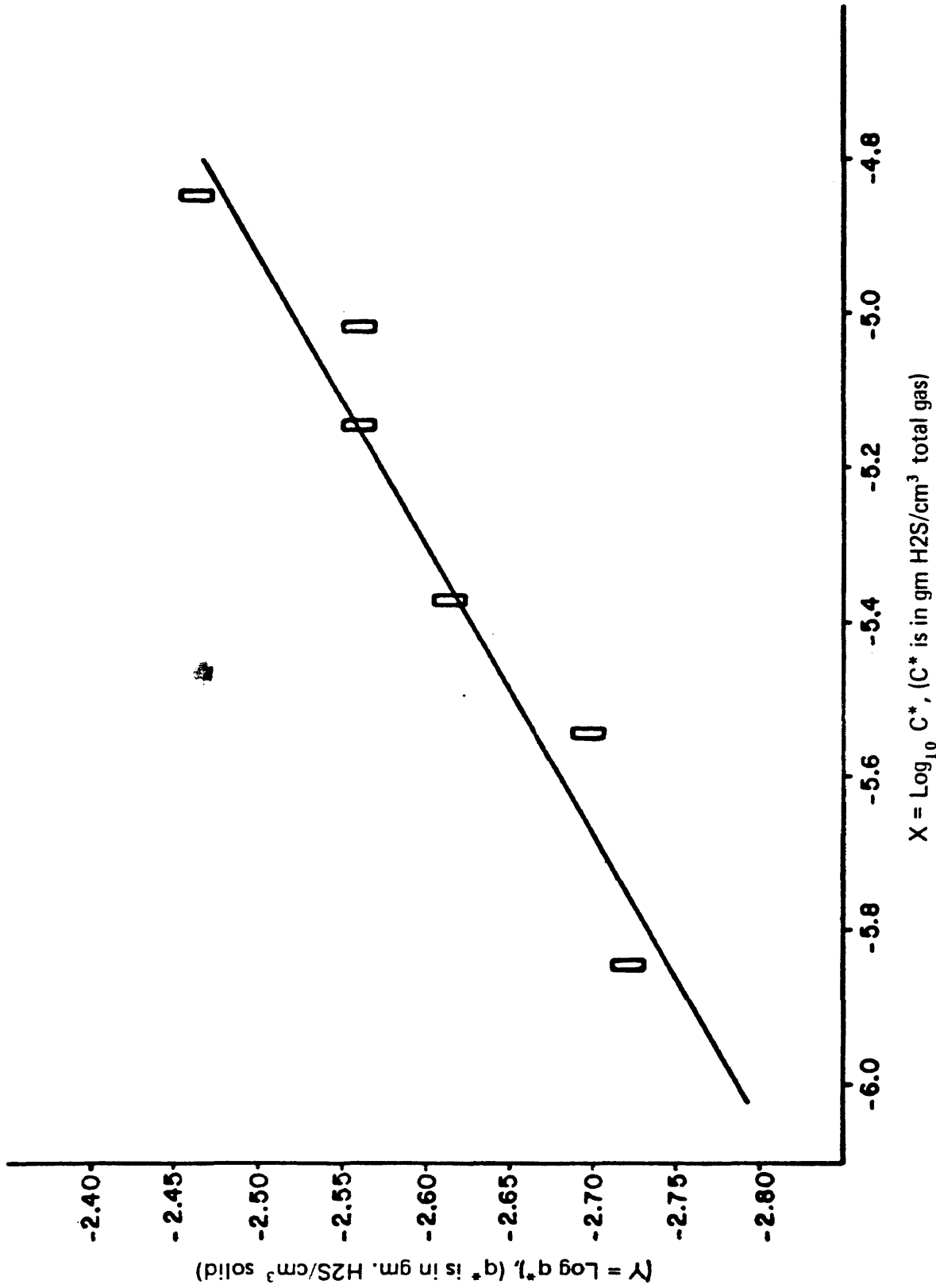


FIGURE 22. ADSORPTION ISOTHERMS OF H₂S ON SPENT SHALE AT 25°C PLOTTED ACCORDING TO THE FREUNDLICH EQUATION (TESTING OF THE FREUNDLICH EQUATION).

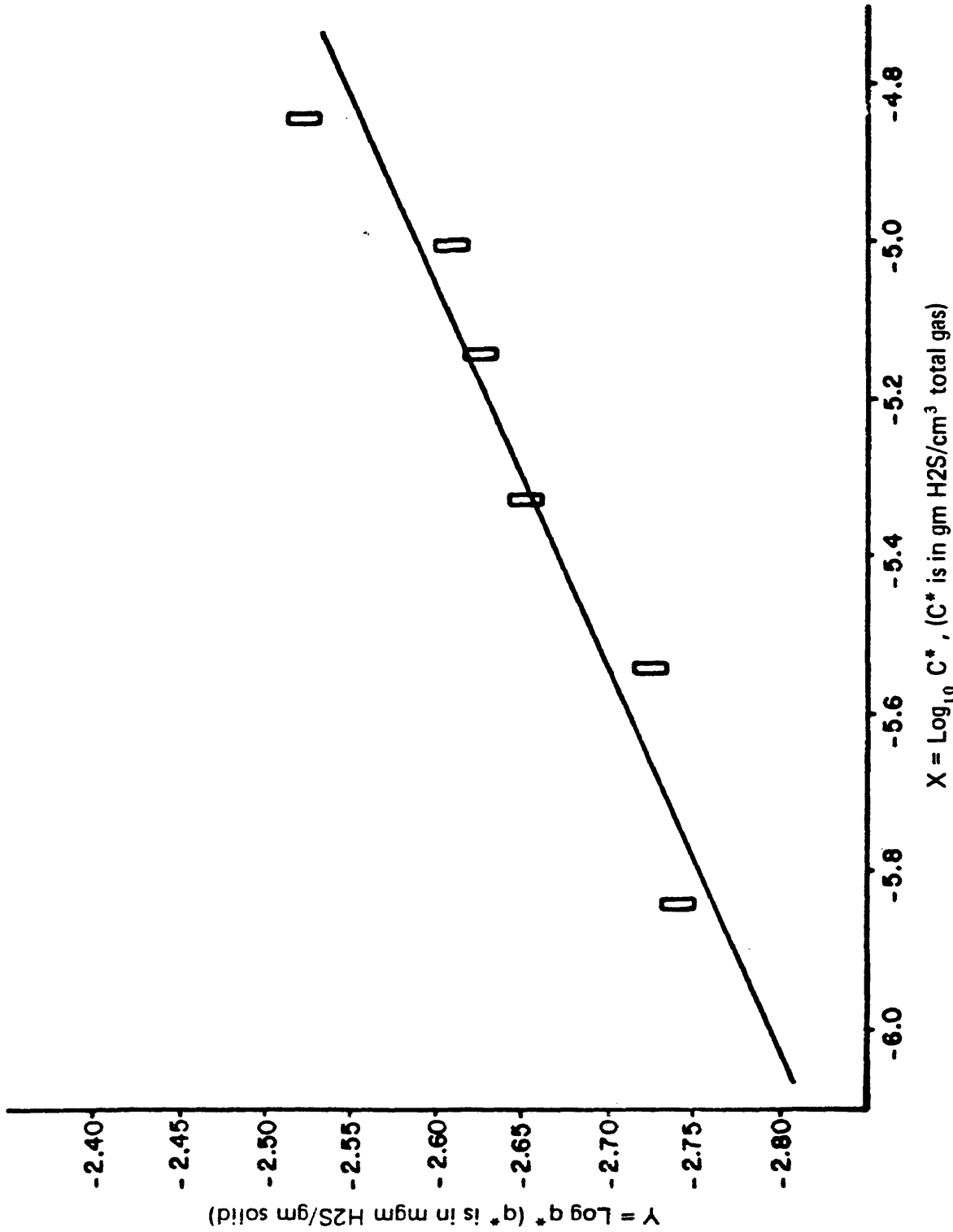


FIGURE 23. ADSORPTION ISOTHERMS OF H₂S ON SPENT SHALE AT 60°C PLOTTED ACCORDING TO THE FREUNDLICH EQUATION (TESTING OF THE FREUNDLICH EQUATION).

In order to calculate characteristic curves from experimental equilibrium data, knowledge of the molar volumes of the sorbed species is required.

The characteristic curves calculated from the equilibrium isotherms are shown in Figure (24). It is apparent that, for each gas, the data of all temperatures lie close to a single characteristic curve as required by the Dubinin-Rolanyi theory. Using the values given in Tables 10, 11, and 12, the equation for a Dubinin isotherm were obtained from least squares analysis (the details of the computer program and the method of calculations which are used for this type isotherm are given in Appendices VI and V, respectively) and are given below for different temperatures:

$$W = 0.14910 e^{-(8.4756 \times 10^{-7}) (\epsilon)^2} \quad \text{for } 10^\circ\text{C} \quad \text{Eq. (39)}$$

$$W = 0.10263 e^{-(5.9639 \times 10^{-7}) (\epsilon)^2} \quad \text{for } 25^\circ\text{C} \quad \text{Eq. (40)}$$

$$W = 0.07626 e^{-(3.8125 \times 10^{-7}) (\epsilon)^2} \quad \text{for } 60^\circ\text{C} \quad \text{Eq. (41)}$$

where W is the volume of the adsorption space.

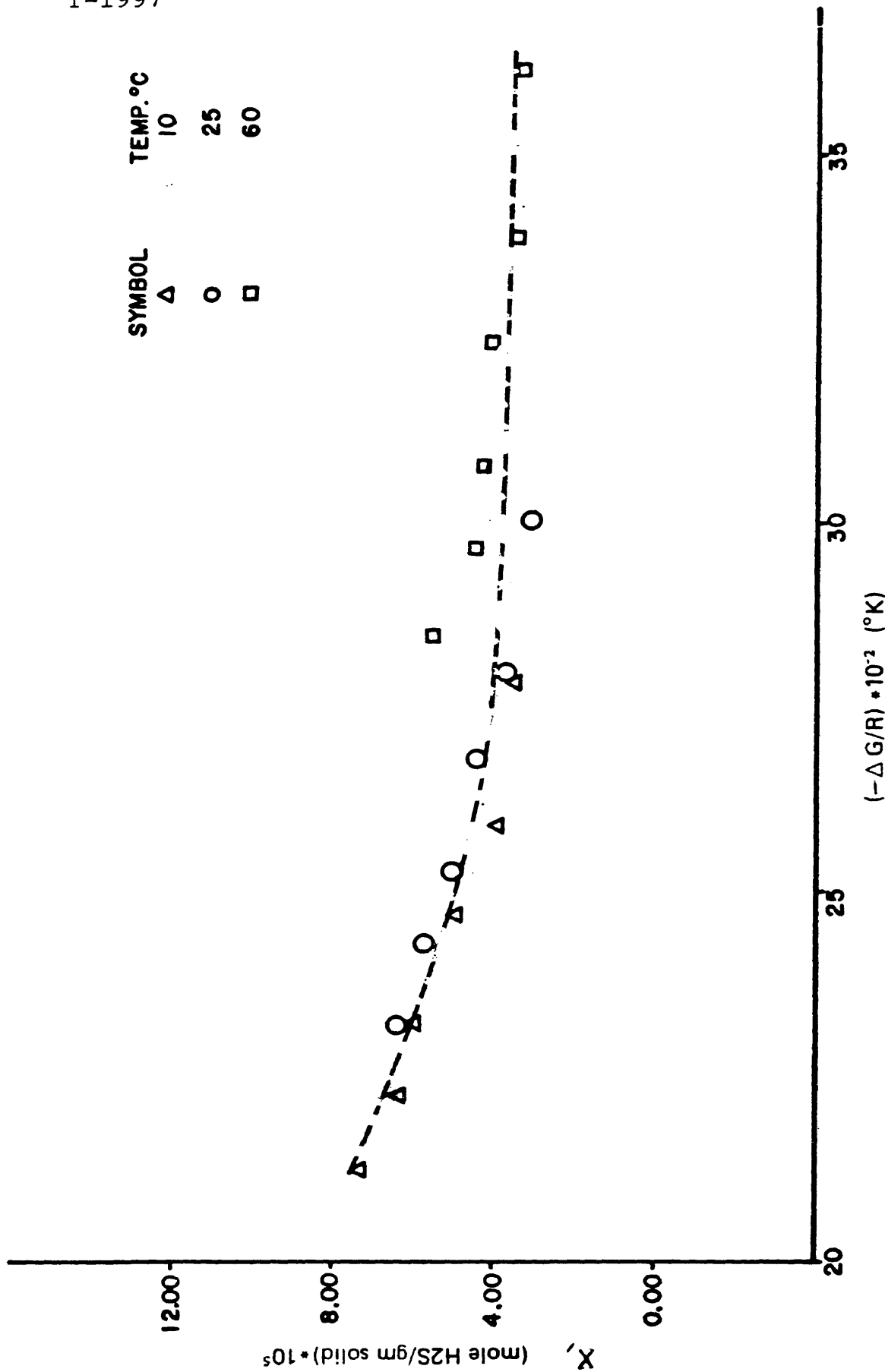


FIGURE 24. CHARACTERISTIC CURVE FOR THE ADSORPTION OF H₂S ON THE SPENT SHALE.

Table 10
Data for Calculation of Polanyi-Dubinin Theory

Concentration H ₂ S in N ₂ , PPM	cm ³ H ₂ S gm solid	Log ₁₀ X, mole H ₂ S gm solid	$\log_{10} \left(\frac{P_0}{P_1} \right)^2$	$c_i = -\Delta G,$ (cal/g mole-°K)	$\frac{(\Delta G)}{R} \times 10^{-3}$ R (°K)	$\frac{(\Delta G)^2}{R} \times 10^{-6}$ R (°K) ²	X, (mole H ₂ S) gm solid x 10 ⁵	mg H ₂ S gm solid
10,000	1.76100	-4.134	10.324	4222.273	2.124	4.51	7.345	2.5032
7,000	1.50969	-4.201	11.343	4425.834	2.227	4.96	6.295	2.1462
5,000	1.44430	-4.220	12.349	4617.862	2.323	5.40	6.026	2.0532
3,000	0.93663	-4.408	15.304	5140.799	2.587	6.69	3.908	1.3315
2,000	0.93663	-4.408	15.304	5140.799	2.587	6.69	3.908	1.3315
1,000	0.83844	-4.456	17.750	5536.386	2.786	7.76	3.499	1.1919

At temperature of 10°C:

C*

Table 11
Data for Calculation of Polanyi-Dubinin Theory

At temperature of 25°C:

Concentration H ₂ S in N ₂ , PPM	C, cm ³ ·H ₂ S gm solid	Log ₁₀ X, mole H ₂ S (X, gm solid)	Log ₁₀ (log ₁₀ (P ₀ /P _i)) ²	ε _i = -ΔG, (cal/g mole-°K)	(ΔG) × 10 ⁻³ R (°K)	(ΔG) ² × 10 ⁻⁶ R (°K) ²	X, (mole H ₂ S) gm solid × 10 ⁵	mg H ₂ S gm solid
10,000	1.53005	-4.193	11.450	4616.923	2.323	5.40	6.412	2.1871
7,000	1.30332	-4.262	12.522	4828.280	2.430	5.90	5.70	1.8630
5,000	1.21532	-4.293	13.577	5027.664	2.530	6.40	5.093	1.7372
3,000	1.07050	-4.356	15.262	5330.366	2.680	7.18	4.406	1.5302
2,000	0.88819	-4.429	16.668	5570.633	2.800	7.84	3.724	1.2696
1,000	0.84711	-4.449	19.217	5981.374	3.010	9.06	3.556	1.2109

Table 12
Data for Calculation of Polanyi-Dubinin Theory

At temperature of 60°C:

Concentration H ₂ S in N ₂ , PPM	C, cm ³ ·H ₂ S gm solid	Log ₁₀ X, (X, $\frac{\text{mole H}_2\text{S}}{\text{gm solid}}$)	$(\text{Log}_{10} \frac{P_0}{P_i})^2$	$\epsilon_i = -\Delta G,$ (cal/g mole-°K)	$\frac{(\Delta G)}{R} \times 10^{-3}$ R(°K)	$\left(\frac{\Delta G}{R}\right)^2 \times 10^{-6}$ R(°K) ²	X, $\frac{\text{mole H}_2\text{S}}{\text{gm solid}}$ x 10 ⁵	$\frac{\text{mg H}_2\text{S}}{\text{gm solid}}$
10,000	1.3099	-4.255	13.810	5665.751	2.85	8.12	5.559	1.895
7,000	1.0729	-4.341	14.985	5901.918	2.97	8.82	4.560	1.5522
5,000	1.0340	-4.357	16.138	6124.708	3.08	9.49	4.395	1.4959
3,000	0.9732	-4.384	17.969	6462.944	3.25	10.56	4.130	1.4079
2,000	0.8213	-4.457	19.493	6731.417	3.39	11.49	3.492	1.1882
1,000	0.7917	-4.473	22.242	7190.374	3.62	13.10	3.365	1.1454

The plot of $\text{Log}X$ versus $[\log_{10} (P_0/P_i)]^2$ gives a straight line for each temperature, with a slope $[2.303 (k/\beta^2)(RT)^2]$ and with the intercept $\text{Log}_{10} (W_0\rho)$. The results are given in Figures (25), (26), and (27), for the three adsorption isotherms. By using the Kagner (2) modification of the Dubinin's equation, the intercept of these plots now will be equal to the logarithm of the monolayer capacity (X_m) rather than the logarithm of the pore volume. So the values of X_m were obtained from these plots and are given below:

$$1) \text{ at } 10^\circ\text{C } \log_{10}(X_m) = -3.67373857, X_m = 2.1196 \times 10^{-4} \frac{\text{mole H}_2\text{S}}{\text{gm solid}}$$

$$2) \text{ at } 25^\circ\text{C } \log_{10}(X_m) = -3.8335920, X_m = 1.4669 \times 10^{-4} \frac{\text{mole H}_2\text{S}}{\text{gm solid}}$$

$$3) \text{ at } 60^\circ\text{C } \log_{10}(X_m) = -3.9573521, X_m = 1.1038 \times 10^{-4} \frac{\text{mole H}_2\text{S}}{\text{gm solid}}$$

The Kaganer treatment yields a method for calculation of specific surface from the isotherm.

The Bet surface area also was obtained as indicated in Table 2.

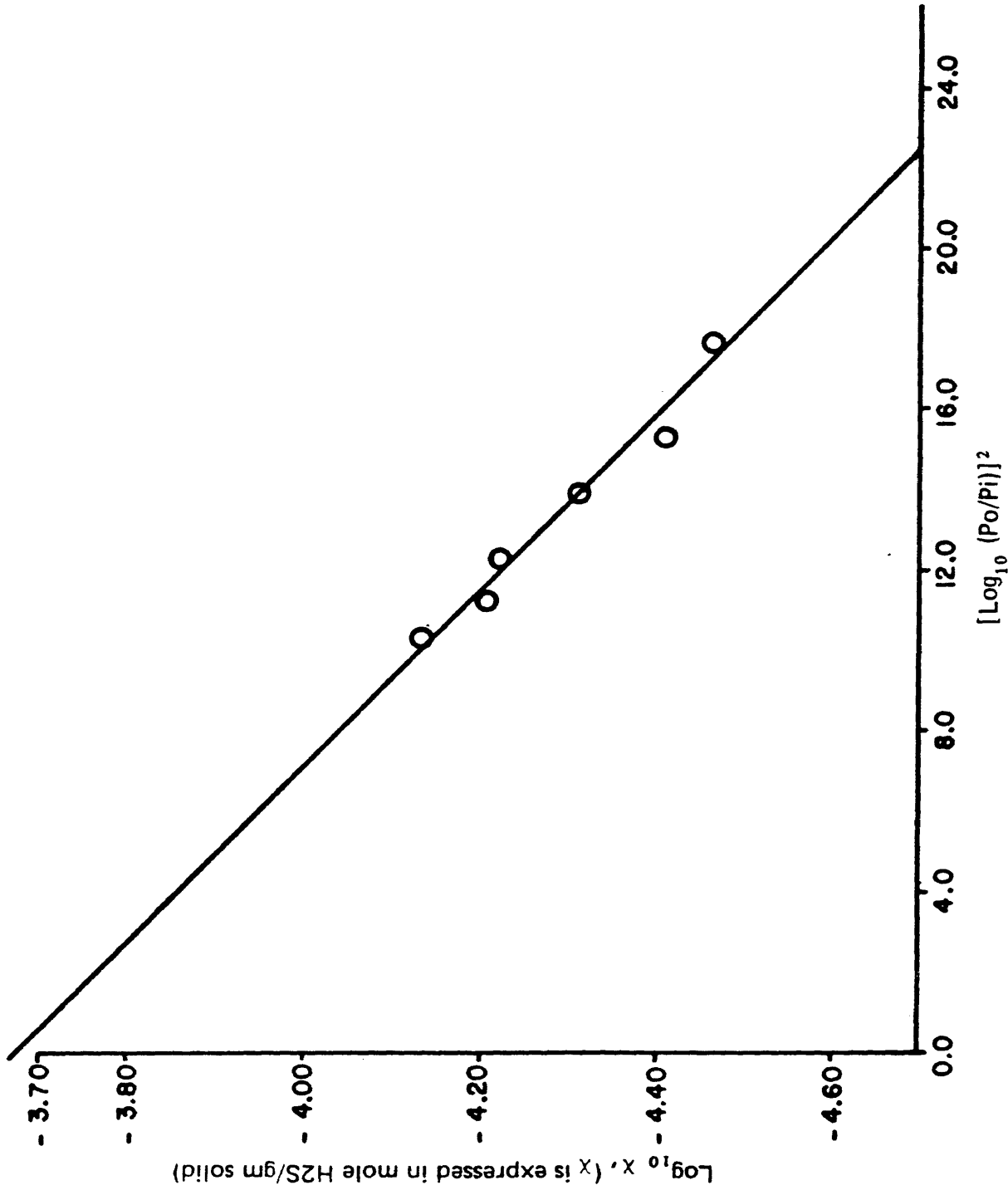


FIGURE 25. PLOT OF LOG X vs. $[\log_{10} (P_0/P)]^2$ FOR THE ADSORPTION OF H₂S at 10°C ON SPENT SHALE PLOTTED ACCORDING TO THE DUBININ EQUATION (POTENTIAL THEORY).

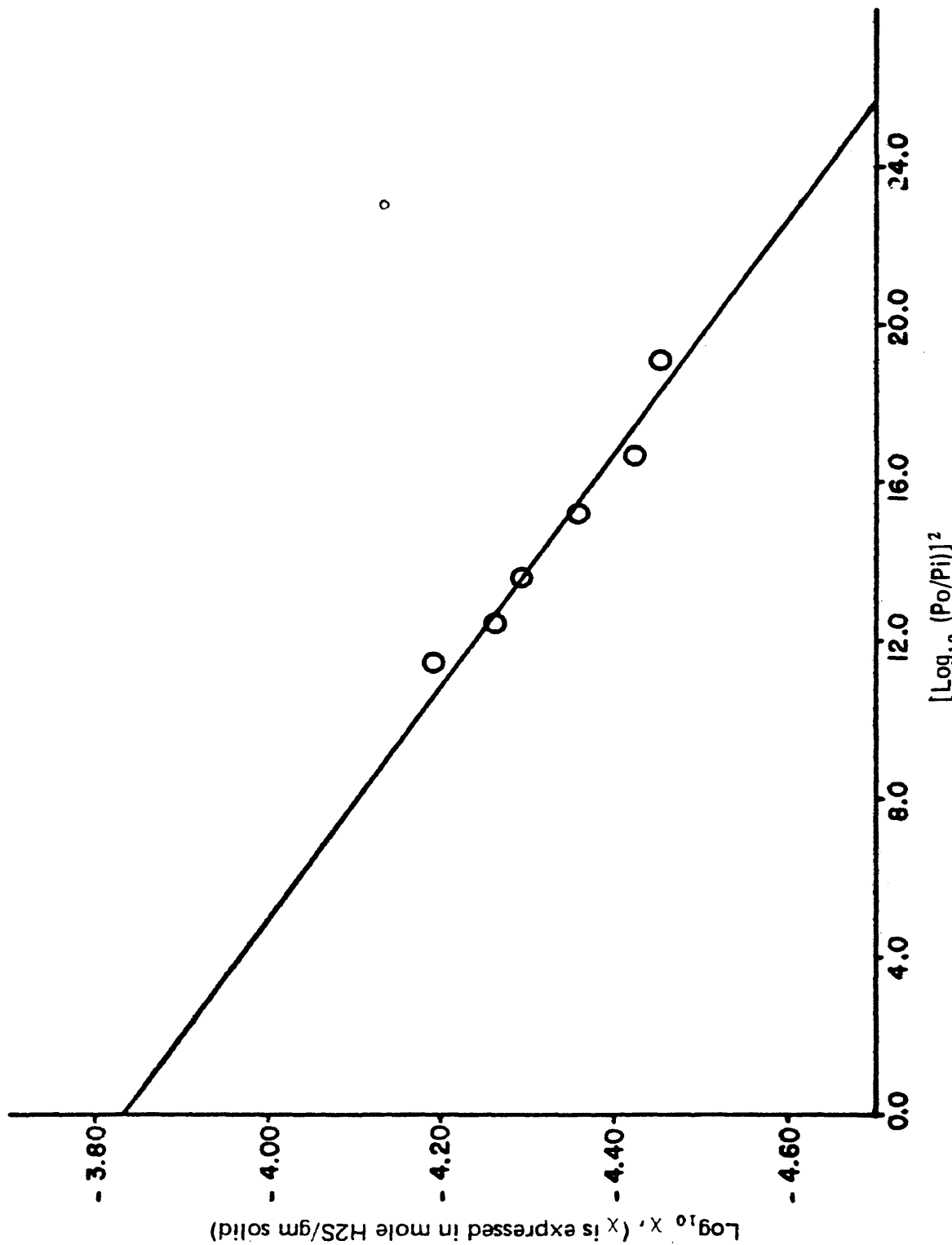


FIGURE 26. PLOT OF $\text{Log } x$ vs. $[\text{Log}_{10} (P_o/P_i)]^2$ FOR THE ADSORPTION OF H_2S AT 25°C ON SPENT SHALE PLOTTED ACCORDING TO THE DUBININ EQUATION (POTENTIAL THEORY).

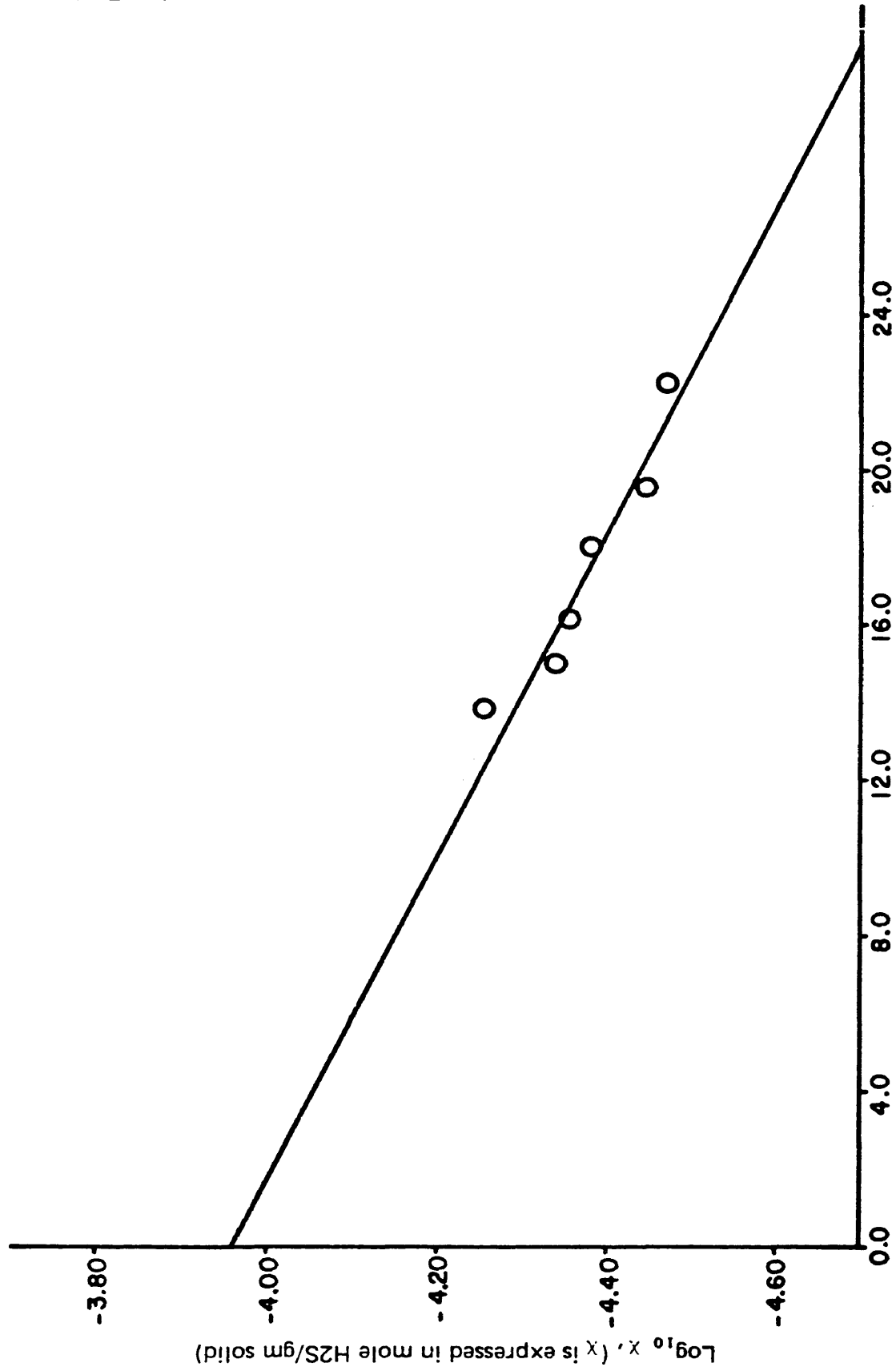


FIGURE 27. PLOT OF $\text{Log } x$ vs. $[\text{Log}_{10} (P_o/P_i)]^2$ FOR THE ADSORPTION OF H_2S AT 60°C ON SPENT SHALE PLOTTED ACCORDING TO THE DUBININ EQUATION² (POTENTIAL THEORY).

Diffusion Coefficients

Internal diffusion models can be used to model the H₂S sorption process with good results. The diffusion coefficients for the diffusion of H₂S on the spent shale were calculated by means of computer (12) generated breakthrough curves using the Langmuir isotherms. The numerical results were plotted on semilog paper with the ordinate $\phi = C/C_0$ while the abscissa was θ/η with the parameters η . For each experimental run $\phi = C/C_0$ was plotted as a function of time (θ_T/η) on semilog paper to the same scale as the theoretical curves for a specific value C_0Q_1 . The theoretical breakthrough curves are shown in Figures (28) through (30) for three different values of C_0Q_1 . The values of C/C_0 vs. θ/η for the theoretical breakthrough curves are given in Appendix VIII. These theoretical curves were then matched to the experimental data to provide information on the sorption mechanism as well as the diffusion coefficients. The model used assumed Langmuir type isotherms which fit the experimental isotherms relatively well.

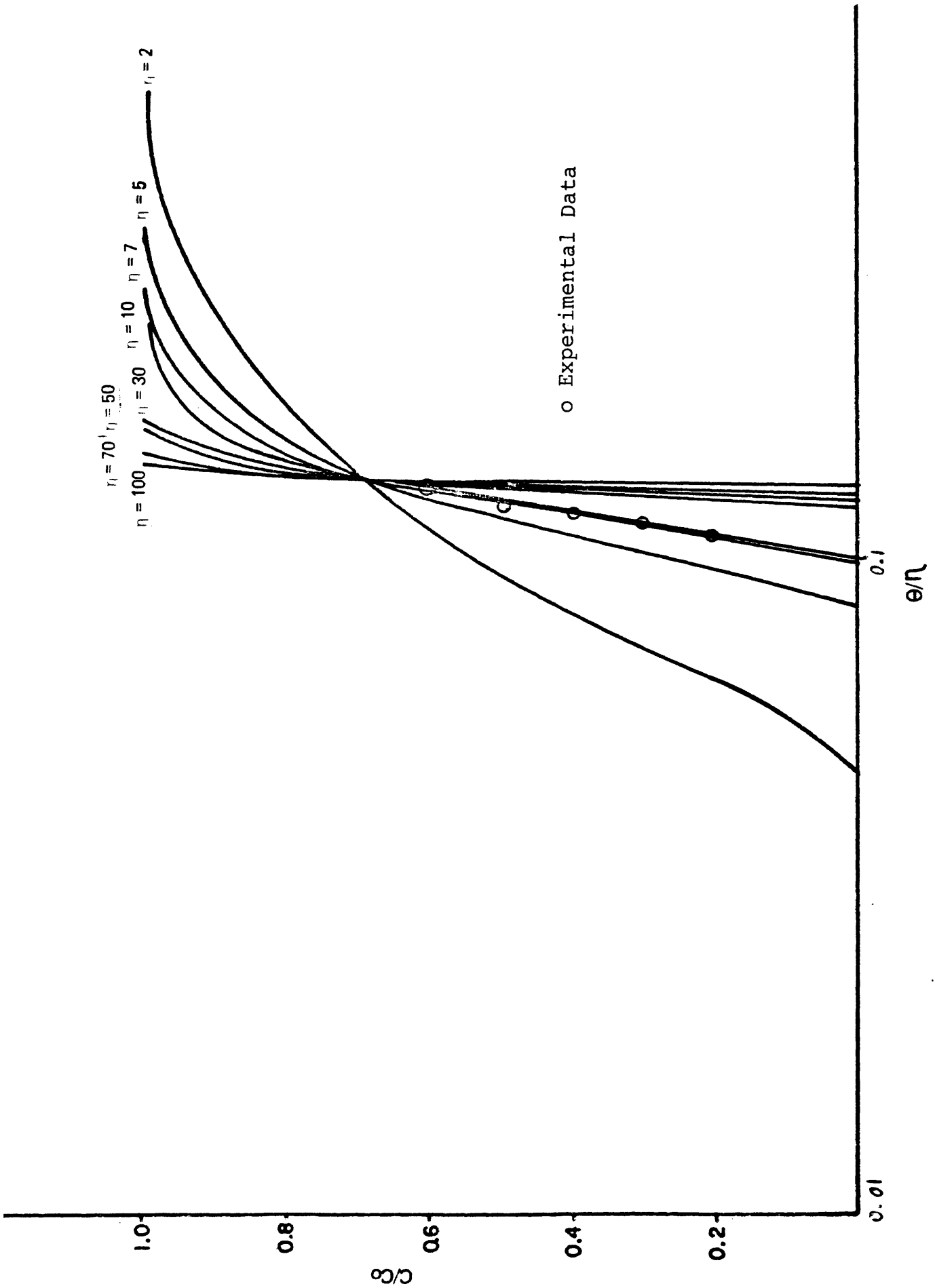


FIGURE 28. THE THEORETICAL BREAKTHROUGH CURVE FOR $Q_1 C_0 = 4.03$.

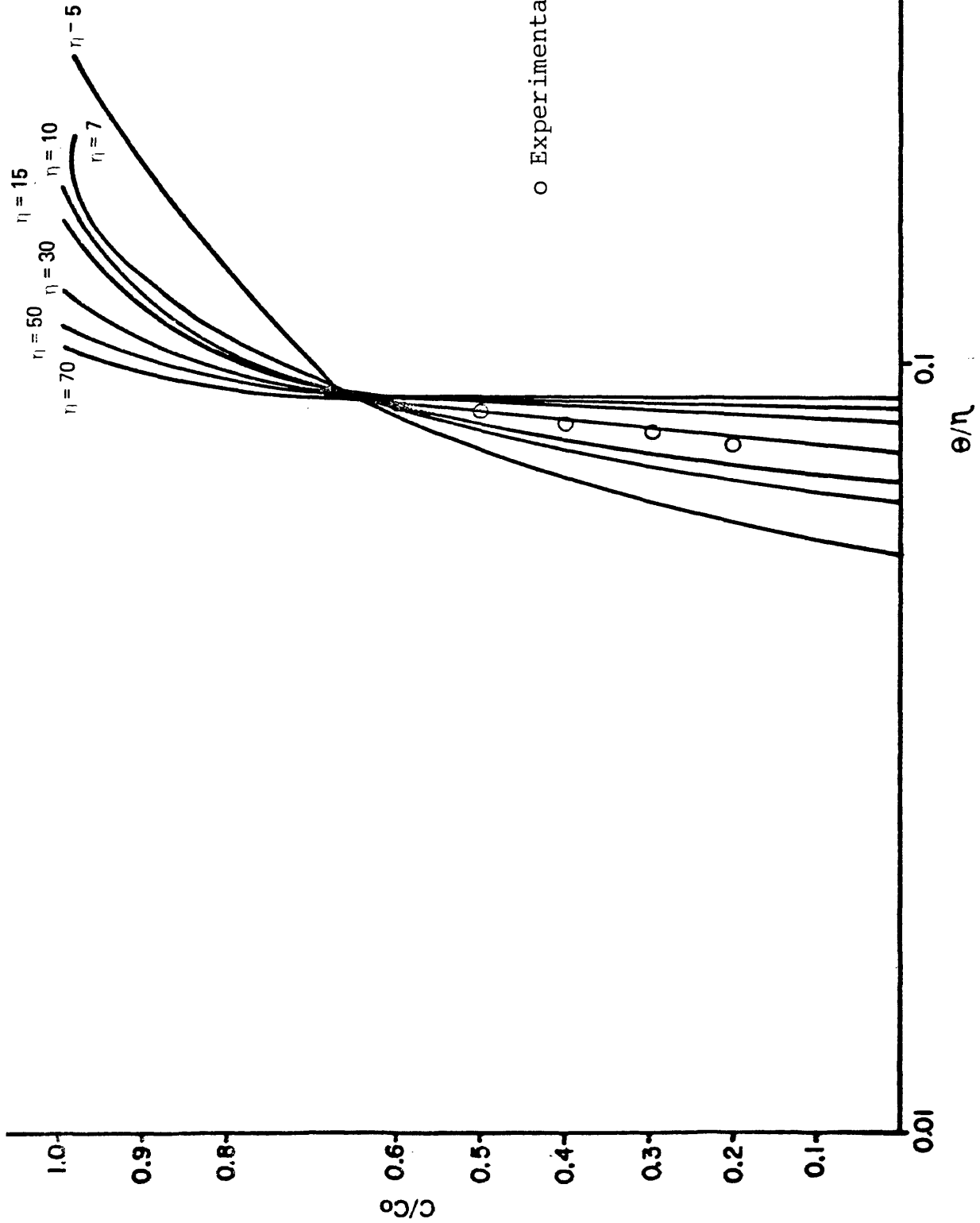


FIGURE 29. THE THEORETICAL BREAKTHROUGH CURVE FOR $Q_1C_0 = 6.12$.

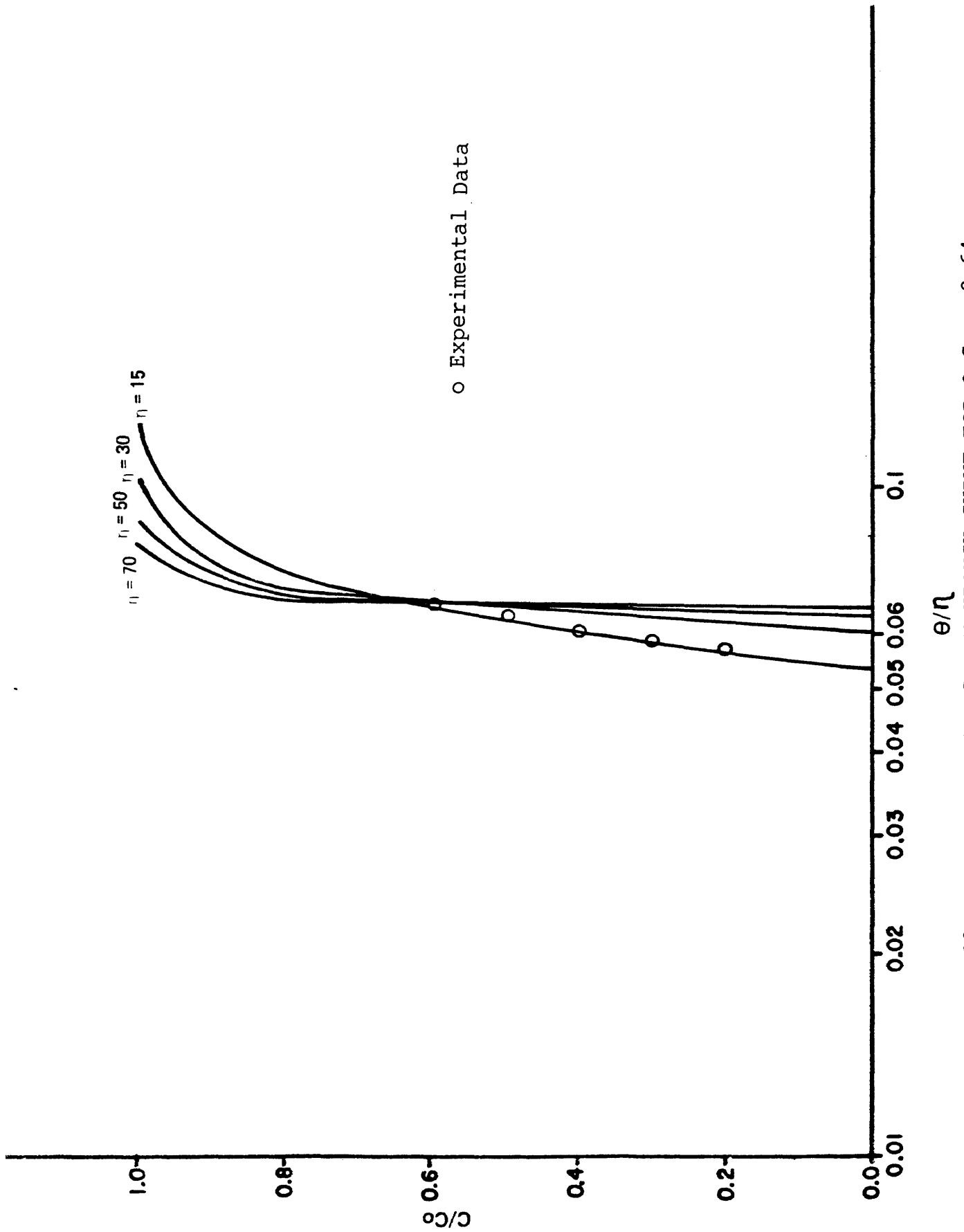


FIGURE 30. THE THEORETICAL BREAKTHROUGH CURVE FOR $Q_1 C_0 = 8.64$.

The method which was used to calculate the overall intraparticle diffusion coefficient will be discussed below. The corresponding value of θ (minute) should be found on the experimental breakthrough curve at a fixed value of temperature and concentration. Upon substituting the values for m , v , Z , Q_0 , and θ (θ from experimental) into equation (30).

$$\theta_T/\eta = (2 m v/3 Q_0 Z) \theta \quad \text{Eq. (30)}$$

The experimental plots of θ_T/η vs. C/C_0 were matched to theoretical breakthrough curves. Then the corresponding value of η was found from the plot $\log (\theta/\eta)$ versus C/C_0 . Substituting the value of η and m , v , R_1 , Q_0 , and Z in Equation (31) gives

$$D = (M V R_1^2/3 Q_0 Z) \eta \quad \text{Eq. (31)}$$

Diffusion coefficients were obtained at three different temperatures 10°C, 25°C, and 60°C for the concentrations of 1000, 5000, and 10,000 PPM H₂S in nitrogen. These results are shown in Tables 13, 14, and 15.

A comparison of the effective diffusion coefficients are plotted at 10°C, 25°C, and 60°C in Figure (31).

Table 13

Diffusion Coefficients at 10°C on Spent Shale for
Concentrations of 1000, 5000, and 10,000 PPM of H₂S in
Dry Nitrogen

C/CO	C*, PPM	$C^* \frac{\text{gm H}_2\text{S}}{\text{cm}^3 \text{ total gas}}$	θ (min)	θ_T/η	η	$D(\text{cm}^2/\text{sec})10^5$
0.2	10,000	14.22×10^{-5}	24.7	0.068	25	5.70
0.3	"	"	24.7	0.068	--	
0.4	"	"	25.4	0.070	--	
0.5	"	"	26.0	0.071	--	
0.6	"	"	27.3	0.075	--	
0.2	5,000	7.11×10^{-5}	37.7	0.112	10	2.41
0.3	"	"	39.0	0.116	--	
0.4	"	"	39.7	0.118	--	
0.5	"	"	40.3	0.120	--	
0.6	"	"	42.9	0.128	--	
0.2	1,000	1.42×10^{-5}	128.7	0.322	7.0	1.42
0.3	"	"	131.3	0.329	--	
0.4	"	"	135.2	0.339	--	
0.5	"	"	140.4	0.352	--	
0.6	"	"	148.8	0.373	--	

Table 14

Diffusion Coefficients at 25°C on Spent Shale for Concentrations of 1000, 5000, and 10,000 PPM of H₂S in Dry Nitrogen

C/Co	C*, PPM	C*, $\frac{\text{gm H}_2\text{S}}{\text{cm}^3 \text{ total gas}}$	θ (min)	θ_T/η	η	$D(\text{cm}^2/\text{sec})10^5$
0.2	10,000	14.29x10 ⁻⁵	21.45	0.049	40	6.79
0.3	"	"	22.10	0.046	--	--
0.4	"	"	22.75	0.047	--	--
0.5	"	"	23.40	0.049	--	--
0.6	"	"	24.70	0.051	--	--
0.2	5,000	7.15x10 ⁻⁵	33.80	0.078	13	2.43
0.3	"	"	35.10	0.081	--	--
0.4	"	"	35.90	0.083	--	--
0.5	"	"	37.50	0.086	--	--
0.6	"	"	39.00	0.090	--	--
0.2	1,000	1.43x10 ⁻⁵	118.30	0.273	10	1.80
0.3	"	"	123.50	0.285	--	--
0.4	"	"	127.40	0.294	--	--
0.5	"	"	132.60	0.306	--	--
0.6	"	"	140.40	0.324	--	--

Table 14

Diffusion Coefficients at 60°C on Spent Shale for Concentrations of 1000, 2000, 5000, and 10,000 PPM of H₂S in Dry Nitrogen

C/Co	C*, PPM	C*, $\frac{\text{gm H}_2\text{S}}{\text{cm}^3 \text{ total gas}}$	θ (min)	θ_T/η	η	D (cm ² /sec) 10 ⁵
0.2	10,000	14.47x10 ⁻⁵	17.5	0.032	5.0	7.39
0.3	"	"	18.2	0.033	--	--
0.4	"	"	18.2	0.033	--	--
0.5	"	"	18.8	0.034	--	--
0.6	"	"	20.1	0.036	--	--
0.2	5,000	7.23x10 ⁻⁵	25.1	0.057	17.5	3.19
0.3	"	"	26.0	0.059	--	--
0.4	"	"	27.3	0.061	--	--
0.5	"	"	28.6	0.064	--	--
0.6	"	"	30.5	0.068	--	--
0.2	1,000	1.45x10 ⁻⁵	114.7	0.214	15	1.99
0.3	"	"	120.9	0.225	--	--
0.4	"	"	126.2	0.235	--	--
0.5	"	"	133.2	0.248	--	--
0.6	"	"	141.7	0.263	--	--

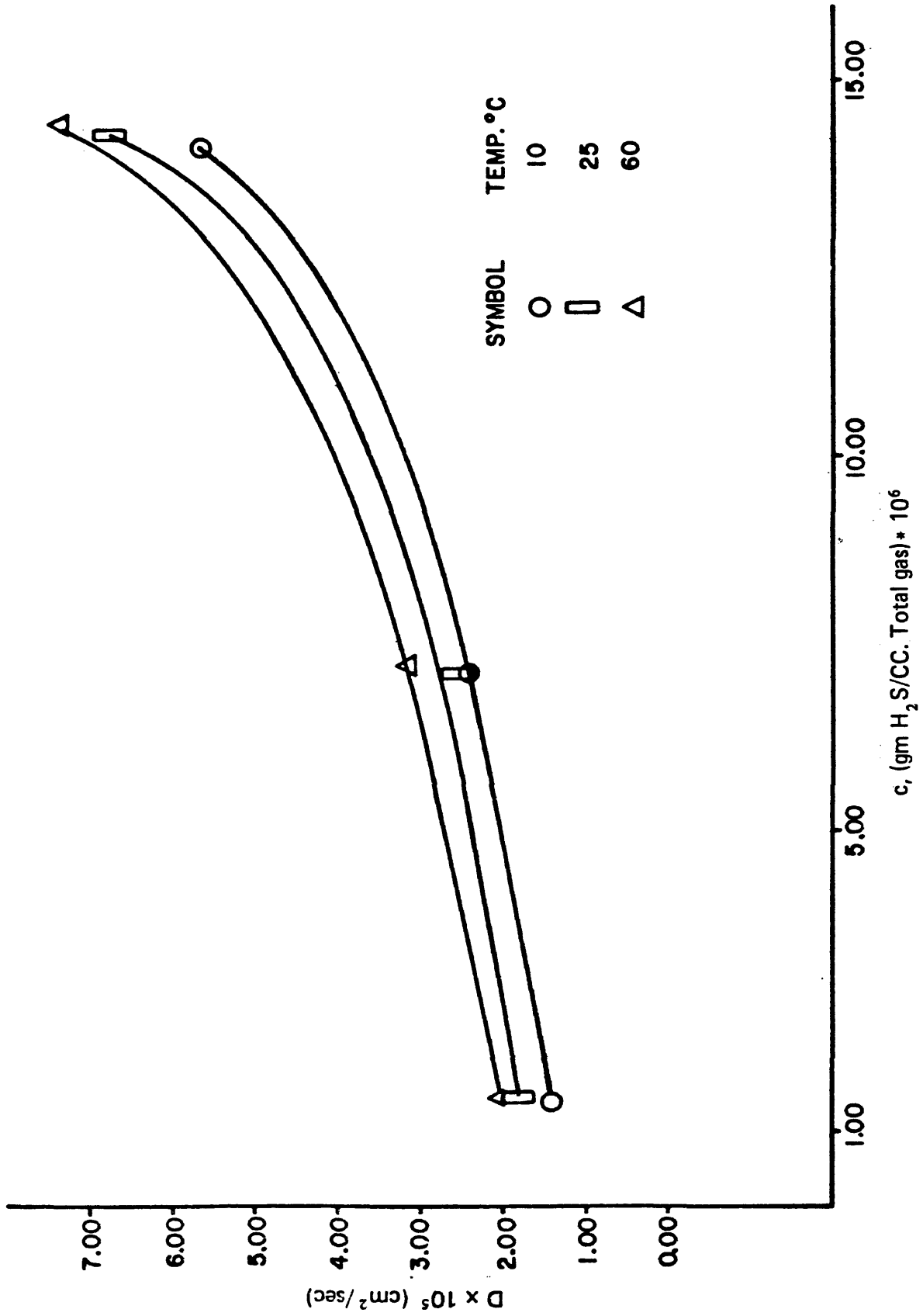


FIGURE 31. COMPARISON OF DIFFUSION COEFFICIENTS AT 10, 25, AND 60°C.

Energy of Activation

Empirically, the diffusion coefficient, D , can be described by the equation

$$D = D_0 \exp \left(- \frac{Q}{RT} \right) \quad \text{Eq. (44)}$$

where D_0 and Q may vary with composition but are independent of temperature. Experimentally D_0 and Q are obtained by plotting $\ln D$ vs. $1/T$, the slope of this plot gives

$$\frac{d \ln D}{d (1/T)} = - Q/R \quad \text{Eq. (45)}$$

while $\ln D_0$ is given by the intercept at $1/T = 0$.

The plots of Log intraparticle diffusivity versus inverse temperature ($^{\circ}\text{K}$) for concentrations of 10,000, 5,000, 1,000 PPM are shown in Figure (32). The best line through the experimental data is obtained by the method of least squares. The slope of this line is $(- Q/R)$, while the intercept is $(\ln D_0)$.

Table 16

Experimental Parameters of Eq. 44

Concentrate in PPM	When $1/T=0$ (D_0)	The slope of the curve $-Q/R$	$D = D_0 \exp(-Q/RT)$
10,000	2.9×10^{-4}	-454.6	$D = 2.9 \times 10^{-4} \exp\left(\frac{-454.6}{T}\right)$
5,000	1.1×10^{-4}	-439.2	$D = 1.1 \times 10^{-4} \exp\left(\frac{-439.2}{T}\right)$
1,000	1.2×10^{-4}	-586.9	$D = 1.2 \times 10^{-4} \exp\left(\frac{-586.9}{T}\right)$

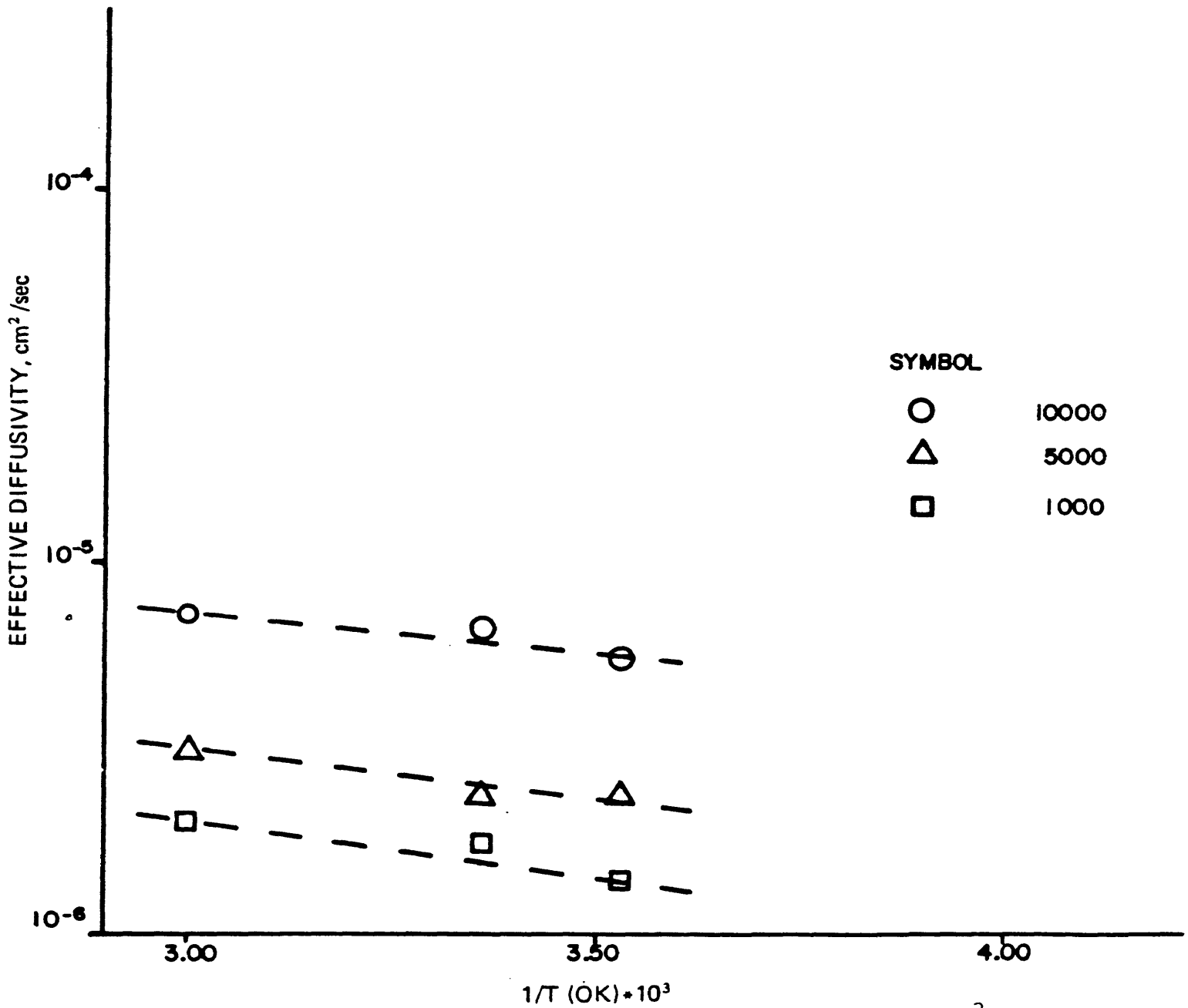


FIGURE 32. EFFECTIVE DIFFUSIVITY vs. (1/T) * 10³.

Heat of Adsorption

The equilibrium data also yields value for the heat of adsorption. Hersh (28) has shown that at constant loading

$$\Delta H_s = - R \left[\frac{\partial (\ln P)}{\partial \left(\frac{1}{T}\right)} \right]_{q^*}$$

Plots of log P vs 1/T can be analyzed graphically for the slope at constant loading in order to obtain ΔH_s .

The heats evolved during the adsorption process were of the same order of magnitude as the heat of condensation, 0.5 to 5 kcal/gmole.

Table 17

The Heats of Adsorption at Different Loading Points

$\frac{q^*, \text{ gm H}_2\text{S}}{\text{cm}^3 \text{ solid}}$	ΔH_s Heat of Adsorption cal/gmole
2.3×10^{-3}	1391
2.5×10^{-3}	2305
2.6×10^{-3}	3498

As the loading increases, the heat of adsorption also increases. This is probably due to a combination of physical adsorption and chemisorption.

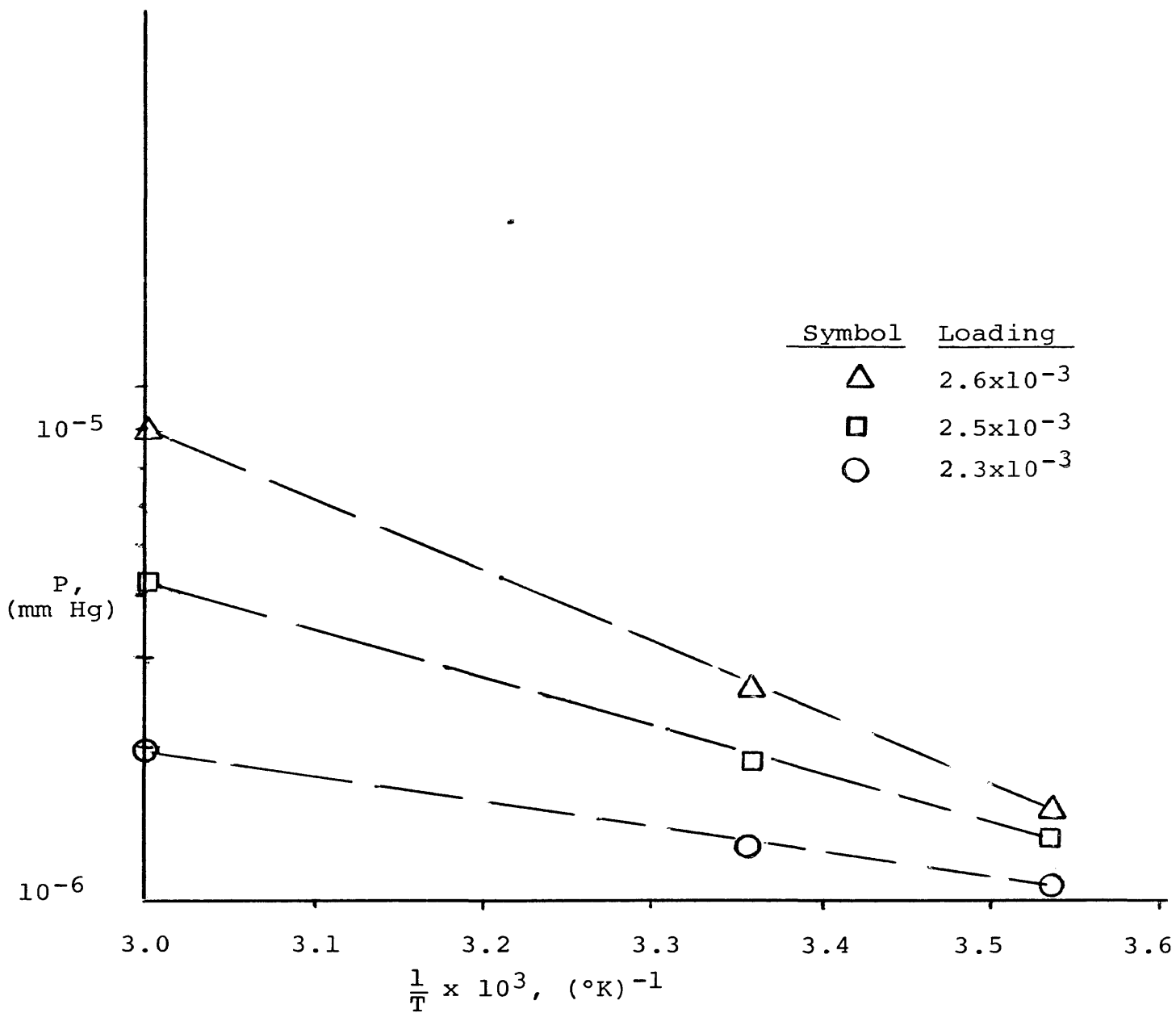


Figure (33). Equilibrium Isosteres for Calculations Heat Adsorption.

CONCLUSIONS

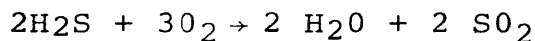
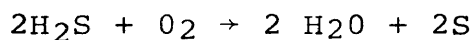
Although the experimental adsorption data could be fit accurately with the Langmuir equations, a better fit was obtained with the Freundlich equation. The experimental data for all isotherms was reduced to a Dubinin-Polanyi type potential plot and were found to obey this type relationship relatively well. The fact that the data could be reduced to a single curve demonstrates the consistency of the data for all temperatures.

The results which were obtained in the previous section indicated that an increase in the diffusion coefficient occurs with an increase at the temperature of adsorption processes.

The desorption curves, which were obtained for each of the runs by passing pure nitrogen at 10, 25, and 60°C through the packed bed, shows that only approximately 10 to 50 percent of the H₂S was recovered. Table 13 presents the percent and amount of H₂S that can be recovered by pure nitrogen in process desorption during the same time period as adsorption. However, upon increasing the temperature to about 40°C above the adsorbing temperature, more than 90 percent of the H₂S could be recovered. It is important to note that for systems, such as this one, in which the diffusion coefficient increases with increasing adsorbate concentration, the desorption process is longer because of diffusion from the adsorbent.

The studies by Compson and Rowan (13) show that H₂S and oxygen react at temperatures well below the H₂S air ignition temperature when oil shale is present.

The reaction products are solid sulfur-containing compounds, including elemental sulfur, and sulfur dioxide gas. Temperature and oxygen concentration strongly effect the steady state product distribution. This effect may be due to the stoichiometry of



One-third of the oxygen is required when forming elemental sulfur, and it may be a favored product when O₂ is scarce. The results of studies on effects of temperature, carrier gas, shale sources or conditions, and H₂S and O₂ concentration show that reaction rate is dependent on temperature for a constant amount of H₂S reacted.

However, in the present study oxygen was not added to the spent shale and the only oxygen present was in the form of compounds. Because the heats of adsorption and the energy of activation were relatively low, it may be assumed that the H₂S was held on the surface by a combination of Vander Waals forces and chemisorption.

Table 18

Desorption by Pure Nitrogen
of H₂S spent shale particles at 10°C, 25°C, and 60°C.

Concentration of H ₂ S, PPM	<u>cm³ H₂S</u>	<u>cm³ H₂S</u>	<u>mg H₂S</u>	<u>mg H₂S</u>	%
	<u>gm solid</u> <u>adsorbed</u>	<u>gm solid</u> <u>desorbed</u>	<u>gm solid</u> <u>adsorbed</u>	<u>gm solid</u> <u>desorbed</u>	
<u>For T = 10 C</u>					
10,000	1.7610	0.84146	2.5034	1.19622	47.78
7,000	1.5096	0.56803	2.1462	0.80750	37.62
5,000	1.4443	0.52429	2.0532	0.74533	36.30
3,000	1.1734	0.38889	1.6682	0.55285	33.14
2,000	0.9366	0.27797	1.3315	0.39516	29.68
1,000	0.8384	0.16705	1.1919	0.23748	19.92
<u>For T = 25 C</u>					
10,000	1.5300	0.65106	2.1871	0.43063	42.55
7,000	1.3033	0.50449	1.8630	0.72112	38.71
5,000	1.2153	0.44258	1.7372	0.63262	36.42
3,000	1.0705	0.28187	1.5302	0.40290	26.33
2,000	0.8881	0.22031	1.2696	0.31491	24.80
1,000	0.8471	0.10662	1.2109	0.15240	12.59
<u>For T = 60 C</u>					
10,000	1.3099	0.48889	1.8950	0.70728	37.32
7,000	1.0729	0.32423	1.5522	0.46906	30.22
5,000	1.0340	0.27557	1.4959	0.39867	26.65
3,000	0.9732	0.27033	1.4079	0.39109	27.78
2,000	0.8213	0.13425	1.1882	0.19422	16.35
1,000	0.7917	0.08334	1.1454	0.12057	10.53

NOMENCLATURE

- A = area (cm^2)
- C = gas phase concentration of H_2S , (gm./cm^3)
- $C(X, \theta)$ = effluent concentration of H_2S , (gm./cm^3)
- C_0 = inlet gas concentration of H_2S , (gm./cm^3)
- C^* = equilibrium gas phase concentration of H_2S , (gm./cm^3)
- D = intraparticle diffusivity, (sq. cm./sec.)
- ΔG = adsorption potential, (cal/gmole)
- k = the constant characterizing of the pore size distribution
- M = the molecular weight of inlet gas (gm./gmole)
- m = void fraction of bed divided by particle fraction, (dimensionless)
- m = quantity dependent on T, the constant in Freundlich equation
- n = quantity dependent on T, the constant in Freundlich equation
- q = average concentration of adsorbed H_2S , (gm./cm^3)
- q^* = equilibrium concentration of adsorbed H_2S , (gm./cm^3)
- q_i = the local concentration of adsorbed H_2S in particle, (gm./cm^3)
- Q_0 = first Langmuir constant (dimensionless)
- Q_1 = second Langmuir constant (cm^3/gm)
- P = pressure (mm Hg)

- P_0 = the saturation pressure of pure adsorbate (mm Hg)
 or vapor pressure at atmospheric pressure (mm Hg).
- P_i = partial pressure (mm Hg)
- R = gas constant, cal./ (gmole) ($^{\circ}K$)
- R_1 = the radius of spherical particle, (cm)
- r = the radial coordinate in particle, (cm)
- S_g = pore surface area (of solid) per unit mass
- t = time (min.)
- T = temperature ($^{\circ}K$)
- v = the linear velocity of gas in the bed ($V_0/A \cdot \epsilon$),
 cm./sec.
- V_0 = volumetric flow rate of the gas (cm³/min.)
- W = volume of the gas adsorbed
- W_0 = the total volume of all the micropores
- x = the weight of adsorbed, gm.
- X = (Z/mv), transformed column length variable, min.
- $X(i)$ = the dimensionless column length variable
 ($i = 1, 2, 3$)
- Z = bed height measured from inlet, (cm)
- β = constant ratio and termed by Dubinin the affinity
 coefficient,
- λ = the dummy intergration variable.
- \emptyset = the C/C_0 , dimensionless concentration
- θ = ($t - Z/v$), transformed time variable, (min.)

- $\theta(i)$ = the dimensionless time variable ($i = 1, 2, 3,$)
- θ_T = $\frac{2D}{R_1^2} \theta$, dimensionless
- ρ = density of gas, gm/cm³
- ϵ = the void volume fraction (dimensionless).
- ϵ_i = adsorption potential, (cal/gmole)
- η = $3D Q_0 z/mv R_1^2$ (dimensionless)
-
- $\mu(2)$ = chemical potential of sorbed species at 2
- $\mu(1)$ = chemical potential of sorbed species at 1

BIBLIOGRAPHY

1. Starling, K., "Fluid thermodynamic properties for light petroleum system," Gulf Publishing Co., Houston, 166 (1973).
2. Engineering Science, Inc., "Air Quality Assessment of the Oil Shale Development Program in the Piceance Creek Basin," Federal Energy Adm. Project Independence Blueprint; Potential Future Role of Oil Shale, Prospects and Constraints, pp. 390, Nov., 1974.
3. Habgood, H.W., Can. J. Chem., 36, 1384 (1958).
4. Langmuir, I., J. Amer. Chem. Soc. 40, 1368 (1918).
5. Polanyi, M., Verh. dtsh phys. Ges. 16, 1012 (1914).
6. Polanyi, M., Verh. dtsh phys. Ges. 18, 55 (1916).
7. Dubinin, M.M., Russ. J. Phy. Chem. (English trans.) 697 (1965).
8. Broad, D.N., and Foster, A.G., J. Chem. Soc., 366, (1948).
9. Kaganer, M.G., Zh. Fiz. Khim, 33, 2202 (1959).
10. Emmett, P.H., (ed.) "Catalysis," Vol. 1, Chap. 2, Reinhold Publishing Co., New York, (1954).
11. Emmett, P.H., and Brunauer, S., J. Am. Chem. Soc., 59, 1553 (1937).
12. Antonson, C.R., Ph.D. dissertation, Northwestern Univ., Evanston, Ill. (1968).
13. Compton, L.E., and Rowan, W.E., "Hydrogen sulfided rempral from retort off-gases using oil shale," American Institute of Chemical Engineers, New York, Vol. 1 (1977).
14. Antonson, C.R., M.S. dissertation, Northwestern Univ., Evanston, Ill. (1966).

15. Antonson, C.R., and Dranoff, J.S., Chem. Eng. Progr. Symp. Ser. Vol. 65, 20, 27 (1969).
16. Brunauer, S., "The adsorption of gases and vapors," Clarendon Press, Oxford, and Princeton University Press, Princeton (1945).
17. Brunauer, S., Emmett, P.H., and Teller, E., J. Am. Chem. Soc., 60, 309 (1938).
18. de Boer, J.H., "The dynamical character of adsorption," Clarendon Press, Oxford (1968).
19. Gregg, S.J., and Sing, K.S.W., "Adsorption, surface area and porosity," Academic Press, London and New York (1967).
20. Hines, A.L., and Sloan, E. Dendy, "The role of spent shale in oil shale, processing and the management of environmental residues," Colorado School of Mines, Golden (1976).
21. Hatfield, J.A., Murphy, C.L., and Hines, A.L., "Adsorption of SO_2 on Peanut Hulls," Proceedings of 3rd National Conference on Complete Water-reuse, 212-216, Cincinnati (1976).
22. Rosen, J.B., J. Chem. Phys., 20, 387 (1952).
23. Smith, J.M., "Chemical engineering kinetics," McGraw-Hill Book Company, New York, 2nd ed. (1970).
24. Shewman, P.G., "Diffusion in solids," McGraw-Hill Book Company, New York (1963).
25. Treybal, R.E., "Mass-transfer operations," McGraw-Hill Book Company, New York, 2nd ed. (1968).
26. Tison, P.R., J. Chem. and Eng. Data, Vol. 7, No. 3, 405 (1962).
27. Culbertson, W.J., Jr., Nevens, T.D., and Hollingshead, R.D., "Disposal of oil shale ash," Colorado School of Mines Quarterly, 65, (4), 89 (1970).
28. Hersh, C.K., "Molecular Sieves," Reinhold, New York (1961).
29. Kondis, E.F., and Dranoff, J.S., A.I.Ch.E. Symposium Series, 117, Vol. 67, p. 25 (1971).

APPENDIX I

Sample Calculation for BET Surface Area

$$\alpha = 1.09 \left[\frac{M}{N_0 \rho} \right]^{2/3}$$

$$\alpha = \left[\frac{34}{6.02 \times 10^{23} \times 1.4216 \times 10^{-3} \times 34} \right]^{2/3}, \quad \rho = 1.4216 \frac{\text{gm}}{\text{lit}}$$

$$\alpha = 1.213 \times 10^{-14} \text{ Cm}^2 = 1213.12 \text{ \AA}^2$$

$$S_g = \left[\frac{V_m N_0}{V} \right] \alpha \quad \text{or} \quad S_g = \frac{6}{\rho \frac{dP}{P}}$$

$$S_g = \left[\frac{6.02 \times 10^{23}}{22400} \right] 1.213 \times 10^{-14} V_m$$

$$S_g = 3.26 \times 10^5 V_m \text{ Cm}^2/\text{g solid adsorbent}$$

V_m , the volume of one monomolecular layer of gas. If V_m is based on a 1.0 gram sample. Then S_g is the total surface per gram of solid adsorbent.

$$P_0 = 10125.594 \text{ mm Hg}, \quad P = 620 \text{ mHg}, \quad P_i = P Y_i$$

$$Y_i = \frac{C^*}{10^6} \text{ (PPM)}, \quad \frac{P_i}{P_0} = 620 \left(\frac{C^*}{10^6} \right) \left(\frac{1}{10125.594} \right)$$

According to the Brunauer-Emmett-Teller equation, the plot of $\frac{P}{V(P_0 - P)}$ vs P/P_0 which was straight-line, was obtained.

Figure (32), and the slope and intercept were obtained for each case from the curve.

$$I = \text{intercept} = 0.00$$

$$S = \text{slope} = 0.57111$$

$$V_m = \frac{1}{S+I} = 1.75097 \text{ Cm}^2/\text{g cat.}$$

$$S_g = 4.35 \times 10^4 V_m$$

$$S_g = 4.35 \times 10^4 \times 1.75 = 7.6167 \times 10^4 \text{ Cm}^2/\text{g cat.}$$

$S_g = 7.61673 \text{ Cm}^2/\text{g cat.}$ The surface area for the spent shale retorted at 750°C .

APPENDIX I I

Details of the computer program for Langmuir type of isotherms.

```

TY PEH1
[12:13:25]
00100      READ(1,1)N,T
00200      WRITE(4,7)T
00300      7  FORMAT(///1X,'***** FOR T= ',F,5X,'*****'////
00400      1 10X,'(1/C*)',15X,'(1/Q)')/////
00500      AN=N
00600      SUMX=0.0
00700      SUMY=0.0
00800      SUMXY=0.0
00900      SUMXX=0.0
01000      DO 2 I=1,N
01100      C  C IS IN cm. /CC.TOTAL GAS, Q IS IN (cm. H2S/CC. SOLID)
01200      READ(1,3)C,Q
01300      X=(1./C)
01400      Y=(1./Q)
01500      WRITE(4,6)X,Y
01600      6  FORMAT(1X,E20.8,5X,E20.8)
01700      SUMX=SUMX+X
01800      SUMY=SUMY+Y
01900      SUMXY=SUMXY+X*Y
02000      2  SUMXX=SUMXX+X**2
02100      XAV=SUMX/AN
02200      YAV=SUMY/AN
02300      CSCF=SUMXY-SUMX*SUMY/AN
02400      CSS=SUMXX-SUMX**2/AN
02500      B=CSCF/CSS
02600      A=YAV-B*XAV
02700      WRITE(4,4)A,B
02800      Q0=1/B
02900      Q1=A*Q0
03000      WRITE(4,5)Q0,Q1
03100      STOP
03200      1  FORMAT(I,F)
03300      3  FORMAT(2F)
03400      4  FORMAT(1X,'A=',E20.8,5X,'B=',E20.8// NOTE THAT THE LANGMIR
03500      1 EQ. IN THE FORM OF LINEAR IS Y=A+B*X '//)
03600      5  FORMAT(1X,'Q0=',E20.8,5X,'Q1=',E20.8//
03700      1 ' NOTE THAT THE LANGMIR EQ. IS IN THE FORM AS
03800      1 Q=(Q0*C/(1+Q1*C))')
03900      END

```

APPENDIX III

Details of the computer program for Freundlich type
of isotherms.

```

TY FED2
[12:14:42]
00100      READ(1,1)N,T
00200      WRITE(4,7)T
00300      7      FORMAT(///1X,'***** FOR T= ',F,5X,'*****'////
00400      1 10X,'(LOG(C*))',10X,'(LOG(Q))'////)
00500      AN=N
00600      SUMX=0.0
00700      SUMY=0.0
00800      SUMXY=0.0
00900      SUMXX=0.0
01000      DO 2 I=1,N
01100      C      C IS IN cm. /CC. TOTAL GAS, Q IS IN (cm. H2S/CC. SOLID)
01200      READ(1,3)C,Q
01300      X=ALOG10(C)
01400      Y=ALOG10(Q)
01500      WRITE(4,6)X,Y
01600      6      FORMAT(1X,E20.8,5X,E20.8)
01700      SUMX=SUMX+X
01800      SUMY=SUMY+Y
01900      SUMXY=SUMXY+X*Y
02000      2      SUMXX=SUMXX+X**2
02100      XAV=SUMX/AN
02200      YAV=SUMY/AN
02300      CSCF=SUMXY-SUMX*SUMY/AN
02400      CSS=SUMXX-SUMX**2/AN
02500      B=CSCF/CSS
02600      A=YAV-B*XAV
02700      WRITE(4,4)A,B
02800      AA=10**A
02900      BB=B
03000      WRITE(4,5)AA,BB
03100      STOP
03200      1      FORMAT(I,F)
03300      3      FORMAT(2F)
03400      4      FORMAT(1X,'A=',E20.8,5X,'B=',E20.8// NOTE THAT THE FRENDLICH
03500      1 EQ. IN THE FORM OF LINEAR IS Y=A+B*X '/')
03600      5      FORMAT(1X,'M=',E20.8,5X,'(1./N)=' ,E20.8//
03700      1 ' NOTE THAT THE FRENDLICH EQ. IS IN THE FORM AS
03800      1 Q=M*(C**(1./N))')
03900      END

```

APPENDIX I V

Details of the computer program for the Dubinin-Polanyi
type of isotherm.

ARTHUR LAKES LIBRARY
COLORADO SCHOOL of MINES
GOLDEN, COLORADO 80401

```

TY PED3
[13:51:28]
00100 READ(1,1)N,T
00200 WRITE(4,7)T
00300 7 FORMAT(//1X, '***** FOR T= ',F,5X, '*****'////
00400 1 10X, '(LOG(P0/P))**2',10X, '(LOG(X))'////
00500 AN=N
00600 SUMX=0.0
00700 SUMY=0.0
00800 SUMXY=0.0
00900 SUMXX=0.0
01000 DO 2 I=1,N
01100 C X IS EXPRESSED IN MOLE H2S /GM. SOLID
01200 READ(1,3)X,Y
01300 WRITE(4,6)X,Y
01400 6 FORMAT(1X,E20.8,5X,E20.8)
01500 SUMX=SUMX+X
01600 SUMY=SUMY+Y
01700 SUMXY=SUMXY+X*Y
01800 2 SUMXX=SUMXX+X**2
01900 XAV=SUMX/AN
02000 YAV=SUMY/AN
02100 CSCP=SUMXY-SUMX*SUMY/AN
02200 CSS=SUMXX-SUMX**2/AN
02300 B=CSCP/CSS
02400 A=YAV-B*XAV
02500 WRITE(4,4)A,B
02600 STOP
02700 1 FORMAT(1,F)
02800 3 FORMAT(2F)
02900 4 FORMAT(1X, 'A=',E20.8,5X, 'B=',E20.8// NOTE THAT THE DUBININ
03000 1 EQ. IN THE FORM OF LINEAR IS Y=A+B*X '//
03100 1 ' NOTE THAT THE DUBININ EQ. IS IN THE FORM AS '//
03200 1 W=W0*((e)**(-k*(E/B)**2)),WHERE:'// E=R*T*LOG(P0/P),A=LOG(W0*D)
03300 1 '//' AND -B=2.303*(k/B**2)*(RT**2),AND D IS DENSITY')
03400 END

```

APPENDIX V

Sample Calculation - Dubinin-Polanyi Equation

$$\epsilon_i = RT \cdot \ln(P_0/P_i) \quad \text{Eq. (46)}$$

where

$$P_i = P Y_i \quad \text{Eq. (47)}$$

M = 620 mm Hg in experimental conditions

$$Y_i = \frac{C^*, \text{ (in PPM)}}{10^6} \quad \text{Eq. (48)}$$

$$W = \frac{X_i}{\rho} \quad \text{Eq. (49)}$$

where: X_i was in gms H_2S adsorbed per gm solid.

Final equation for the calculation ϵ_i will be such as equation (50) which ϵ_i was in (cal/g-mole),

$$\epsilon_i = R \times T \text{ (}^\circ\text{K)} \ln \left(\frac{P_0}{\frac{(P \times C^*)}{10^6}} \right) \quad \text{Eq. (50)}$$

The adsorption potential ΔG is defined as

$$\Delta G = \mu(2) - \mu(1) = RT \ln \left(\frac{P_0}{P_i} \right) \quad \text{Eq. (49)}$$

for the temperature below the critical temperature.

Example: at 10°C

From the computer program for Dubinin we have this equation

$$Y = -3.67373858 - 0.045445163(X) \quad \text{Eq. (50)}$$

$$A = \text{Log}_{10} (W_0 \rho) = -3.67373858 \quad \text{Eq. (51)}$$

$$\rho = 1.4216 \times 10^{-3} \text{ g/Cm}^3$$

$$-B = 2.303 (RT) \left(\frac{\beta k}{2} \right)$$

$$\left(\frac{k}{\beta^2} \right) = \frac{-B}{2.303 (82.057) (283.73)} = 8.4756 \times 10^{-7}$$

$$\epsilon^2 = (RT \ln \frac{P_0}{P})^2 = (82.057)^2 (283.73)^2 \left(\ln \frac{P_0}{P} \right)^2$$

So the Dubinin equation will be as follows:

$$W = 0.14910 e^{-(8.4756 \times 10^{-7}) (\epsilon)^2}$$

APPENDIX V ISample Calculation - Uptake on H₂S on Spent Shale

$$\text{a) Total cm}^3 \text{ H}_2\text{S adsorbed} = \frac{(\text{Concentration})(\text{Flowrate})}{(\text{height})(\text{speed chart})} \times$$

(area under the breakthrough curve)

$$\text{b) } \frac{\text{cm}^3 \cdot \text{H}_2\text{S adsorbed}}{\text{gm solid}} = \frac{\text{Total cm}^3 \text{ H}_2\text{S adsorbed}}{\text{weight in bed}}$$

Example:

T = 10°C, C₀ = 10,000 PPM, and flowrate - 67.04 cc/min.

$$\left[\frac{(10,000) \text{ cm}^3 \text{ H}_2\text{S}}{10^6 \text{ cm}^3 \text{ gas}} \cdot \frac{67.04 \text{ cm}^3 \text{ gas}}{\text{min}} \right] \frac{1}{(8.30)(0.5 \text{ inch/min})} (145.79) = 23.55 \text{ cm}^3\text{-H}_2\text{S}$$

$$\text{or divide by 13 gms give } \frac{23.55}{13} = 1.81163 \frac{\text{cm}^3\text{-H}_2\text{S}}{\text{gm solid}}$$

APPENDIX VI I

Parameters Used in Calculations

<u>T, Temperature °C</u>	<u>P, Density of H₂S, gm/l</u>	<u>P₀, Vapor pressure of H₂S, mm Hg</u>
10	1.4216	10125.594
25	1.4294	15000.88
60	1.4467	32251.892

The room pressure was 620 mm Hg at the experimental conditions $\rho_s = 1.58$ for spent shale. Reactor cross-sectional area = 0.9369 cm² and inside diameter of reactor = 0.43 inches. Length of sorption reactor was 15.24 cm.

APPENDIX VII I

Values of θ/η vs. C/C_0 for different values of Q_1C_0
for theoretical breakthrough curve (output of program).

APPENDIX IX

Experimental breakthrough curve data at 10°C, 25°C, and 60°C for concentrations of 1000, 2000, 3000, 5000, 7000, and 10,000 PPM. H₂S in dry nitrogen gas.

